M.E. (Water Resources & Hydraulic Engineering) Course affiliated to
Faculty of Engineering and Technology,
Jadavpur University, Kolkata, India

CERTIFICATE OF RECOMMENDATION

This is to certify that the thesis entitled ***"ADSORPTION STUDIES OF PHOSPHATE REMOVAL FROM GROUND AND SURFACE WATER USING LOCALLY AVAILABLE JUTE FIBRE IN WEST BENGAL"*** is bonafide work carried out by **SUMAN BANERJEE** under our supervision and guidance for partial fulfilment of the requirement for Post Graduate Degree of Master of Engineering in Water Resources & Hydraulic Engineering during the academic session 2022-2024**.**

DIRECTOR
School of Water Resources Engineering
Jadavpur University, Kolkata- 700032

THESIS ADVISOR
Prof. (Dr.) Pankaj Kumar Roy
School of Water Resources Engineering
Jadavpur University, Kolkata- 700032

DEAN
Faculty of Interdisciplinary Studies, Law & Management
Jadavpur University, Kolkata- 700032

CERTIFICATE OF APPROVAL **

This foregoing thesis is hereby approved as a credible study of an engineering subject carried out and presented in a manner satisfactorily to warranty its acceptance as a pre-requisite to the degree for which it has been submitted. It is understood that by this approval the undersigned do not endorse or approve any statement made or opinion expressed or conclusion drawn therein but approve the thesis only for purpose for which it has been submitted.

Committee of final examination
For the evaluation of the thesis

**** Only in case the thesis is approved.**

Declaration of Originality and Compliance of Academic Ethics

I hereby declare that this thesis contains literature survey and original research work by the undersigned candidate, as a part of my Master of Water Resources & Hydraulic Engineering degree during academic session 2022-2024.

All information in this document has been obtained and presented in accordance with academic rules and ethical conduct.

I also declare that, as required by this rules and conduct, I have fully cited and referred all material and results that are not original to this work.

Name: *SUMAN BANERJEE*

Roll Number: M2WRE23006

Thesis Title: ***ADSORPTION STUDIES OF PHOSPHATE REMOVAL FROM GROUND AND SURFACE WATER USING LOCALLY AVAILABLE JUTE FIBRE IN WEST BENGAL***

Signature:

Date:

ACKNOWLEDGEMENT

I express my sincere gratitude to my Thesis Advisor **Prof. (Dr.) Pankaj Kumar Roy** under whose valuable guidance this work has been carried out. It would have been impossible to carry out this thesis work with confidence without his wholehearted involvement, advice, support and constant encouragement throughout. He has not only helped me to complete my thesis work but also have given valuable advice to proceed further in my life.

I also express my sincere gratitude to **Prof. (Dr.) Chandan Kumar Ghosh** Assistant Professor, School of Materials Science & Nanotechnology for proving FTIR results. I also express my sincere gratitude to the Department of Physics for providing FESEM and EDX results of the materials.

I also express my thankfulness to Dr. Sudipa Halder, Dr. Swetasree Nag, Shilpa Saha Senior Research Fellow, Priyabrata Mondal Senior research Fellow, Sourav Kumar Basak Senior Research Felow and Pratik Maiti Research Fellow, School of Water Resources Engineering, Jadavpur University for their support throughout the study and also thanks to all my classmates of School of Water Resources Engineering, Jadavpur University, specially, Moumita Paramanik for her helps during thesis work.

Last but not the least; I am also grateful to my parents and my friends for their earnest support.

Date: March, 2024

Place: Jadavpur University, Kolkata

Suman Banerjee
(Roll No. M2WRE23006)

Contents

1 LIST OF TABLES viii

2 LIST OF FIGURES ix

CHAPTER 1 1

2.1 INTRODUCTION 1

2.1.1 Phosphate 1

2.1.2 Sources of Phosphate 2

2.1.3 Effects of varying concentrations of phosphate on human health 3

2.1.4 Phosphate Mitigation strategy 10

3 CHAPTER-2 10

3.1 LITERATURE REVIEW 17

3.1.1 Literature Review 17

3.1.2 Research Gap 20

4 CHAPTER-3 22

4.1 OBJECTIVE & SCOPE OF WORK 22

4.1.1 Objective of the study 22

4.1.2 Scope of the study 22

5 CHAPTER-4 23

5.1 BIOCHAR 23

5.1.1 Application of biochar for phosphate removal 25

5.1.2 Plant/Animal based biochar 26

5.1.3 Agricultural based biochar 26

6 CHAPTER- 5 32

6.1 MATERIAL & METHODS 32

6.1.1 Jute Fibre collection 32

6.1.2 Preparation of jute biochar 32

6.1.3 Stock solution preparation 38

6.1.4 Preparation of Synthetic Solution 27

6.1.5 Method for measuring Phosphate concentration in water 29

6.1.6 Point of Zero Charge 30
6.1.7 Batch Study 30
6.2 ADSORPTION ISOTHERM FOR BATCH EXPERIMENT 31
6.2.1 Langmuir Isotherm 32
6.2.2 Freundlich Model 33
6.2.3 Temkin Isotherm 33
6.3 KINETICS STUDY FOR BATCH EXPERIMENT 34
6.3.1 Pseudo-first-order model 34
6.3.2 Pseudo-second-order model 34
6.3.3 Intra-particle diffusion Model 35
6.4 COLUMN STUDY 36
6.5 ADSORPTION MODELS FOR COLUMN STUDY 40
6.5.1 Bohart–Adams Model 40
6.5.2 Yoon–Nelson Model 40
6.5.3 Thomas Model 41
7 CHAPTER-6 49
7.1 RESULT & DISCUSSION 49
7.1.1 Analysis of phosphate at different concentration 49
7.2 CHARACTERIZATION STUDY OF THE ABSORBENT 49
7.2.1 FESEM & EDX Study 49
7.2.2 FTIR Study 52
7.3 DISCUSSION 53
8 CHAPTER- 7 54
8.1 CONCLUSION & LIMITATION 54
8.1.1 Conclusion 54
8.1.2 Limitation of the study 55
8.1.3 Future works 55
9 REFERENCES 56

LIST OF TABLES

Table 1: Phosphate concentrations in different countries around the world 3

Table 2 Global demand of phosphate fertilizer and mine production of phosphate rock 4

Table 3: Permissible Limits of Phosphate……5

Table 4: Different concentration of phosphates and their consequences……8

Table 5: Plant/Animal based adsorbent 29

Table 6: Agricultural waste based adsorbent 31

Table 7: Modified biochar for phosphate removal 38

Table 8: Comparison of the typical operation conditions for biochar production 42

Table 9: Phosphate Synthetic Stock preparation..... 49

Table 10: Phosphate adsorption at different concentration 52

LIST OF FIGURES

Fig. 1: Phosphate fertilizer use by region 2

Fig. 2: Biochar made from Jute fibre 8

Fig. 3: Jute Fibres of size 2 to 4 mm 32

Fig. 4: Van Krevelen diagram for raw materials and biochars 34

Fig. 5: Comparison of the product distributions of pyrolysis and gasification of biomass 36

Fig. 6: Chopped fibres grinded in mixer grinder 37

Fig. 7: Biochar from Jute 40

Fig. 8: Ion Selective Electrode Method 41

Fig. 9: SEM image of Jute Biochar 50

Fig. 10: EDX graph of Jute Biochar 51

Fig. 11: Fourier Transformation Infrared (FTIR) spectral data of Jute biochar 52

ABSTRACT

Surface water pollution by phosphate has become a significant global concern due to its detrimental effects on aquatic ecosystems and human health. Excessive phosphorus levels lead to algal blooms, oxygen depletion, and eutrophication, endangering aquatic life. Agricultural practices, particularly the widespread use of phosphorus-based fertilizers, contribute significantly to phosphate runoff into water bodies. Additionally, industrial activities and sewage discharge further exacerbate phosphate contamination in rivers and lakes.

Phosphate pollution poses risks beyond environmental degradation, as it can contaminate food sources and contribute to health issues such as hyperphosphatemia and cardiovascular complications. Furthermore, phosphate rocks used in fertilizers contain harmful elements like cadmium and radioactive substances, posing additional threats to the environment and human health.

Various methods have been explored to mitigate phosphate pollution, with adsorption technology emerging as a promising solution. Activated carbon, though widely used, has limitations in phosphate adsorption capacity, prompting research into alternative adsorbents like biochar. Biochar, with its unique physical and chemical properties, exhibits excellent adsorption capabilities for phosphate and other contaminants.

Despite its potential, optimizing biochar's adsorption efficiency requires consideration of factors such as temperature, pH, and contact time. Continued research and development efforts are necessary to harness biochar's full potential in water remediation, offering a sustainable and cost-effective alternative to conventional treatment methods. Literature reviews underscore the growing interest in biochar-based adsorption studies, emphasizing its importance in addressing water pollution challenges globally.

CHAPTER 1

2.1 INTRODUCTION

The surface water pollution by phosphate from a wide variety of sources is a major problem in many parts of the world. Phosphorus, a plant nutrient, excess quantities of it can lead to high growth of phytoplankton, macro-algae and plants. When phosphate concentration is excess in water bodies, there is over growth of water plants which is the cause of formation of algal bloom, it causes dissolved oxygen (DO) consumption in water. Therefore, DO in water bodies reduces very fast, leading to the death of plants and aquatic life. The dead aquatic animals and plants deteriorate the water quality which is termed as Eutrophication [*moshoeshoe2018*]. The total agricultural use of inorganic fertilizers (Nitrogen, phosphorus and potassium) globally was 195 million tonnes in 2021 where as the use of phosphorus as P_2O_5 is 18 to 25 percent of the total in all region[*FAO2023*].

The world population is likely to be increased to 9 billion by 2070 [*lutz2013*]. This would raise demand for food and consequently, for P rock. Unfortunately, mineral fertilizers—which are a valuable source of nutrients for increased food production—have now become "necessary evil." For many years, the overuse of nitrogen and phosphorus fertilisers has resulted in the agricultural soils becoming practically explosive chemical environments [*dissanayake*]. According to the Fig.1, the use of phosphorus as P_2O_5 increases from 2000 to 2021 in Asia and America. Due to the heavy use of phosphates in the form of fertilizer to the agricultural land, the runoff from the lands into the river and the presence of phosphate in sewage water are the main sources of phosphate in river [*almanassra2020*]. In many studies it is found that large number of P are loaded in many major aquatic systems, for instance, about 12.2 kt P was discharged to water bodies in France in 2006 and in Chesapeake Bay (US) it was around 21.7 kt P in 2011 [*chowdhury2017*]. A study in Loktak lake, India found that the phosphate concentration was in the range between 0.002 to 0.8 mg/L and maximum concentration of 8.21 was recorded in Komlakhong North side [*singh2023*]. A study on Ganga River says that atmospheric depositions and concentration of phosphate is also increasing over the time period from 2007 to 2011 in Ganga river [*pandey2013*]. Phosphate

rocks have a wide range of chemical elements that are harmful to the environment, including As, Pb, Hg, and Cd, because of their unique geological and mineralogical nature. Cadmium has been identified as one of the most potentially harmful substances present in phosphate fertilizers after the discovery of the dreaded sickness "Itai-Itai". Consuming large amount of phosphate are responsible for hyperphosphatemia that has been associated with chronic kidney disease and cardiovascular complications in human body. High amounts of naturally occurring radioactive elements from the decay series of uranium and thorium ^{238}U and ^{232}Th can be found in phosphate rocks. The majority of these naturally occurring radionuclides can be found in the solid waste of the phosphate fertilizer industry, including phosphogypsum and radioactive

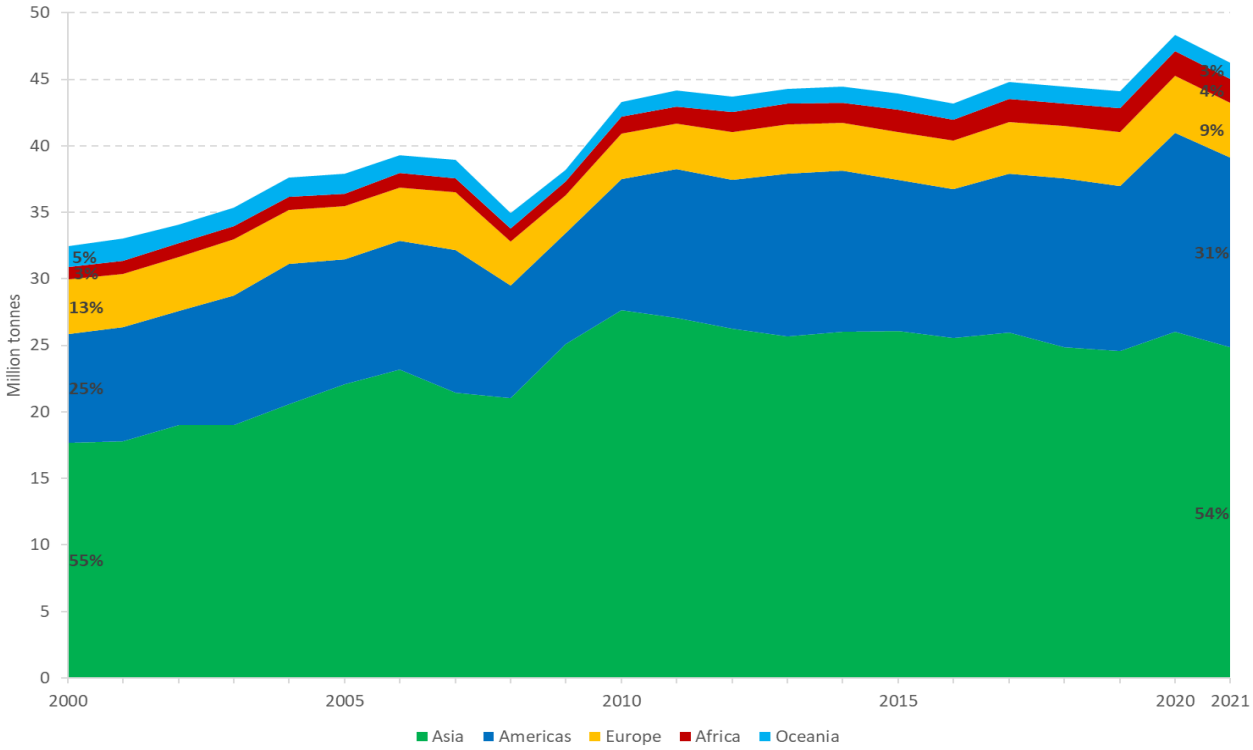


Fig1:Phosphate fertilizer use by region

dust. Many studies have been conducted worldwide to evaluate the risks to the environment and to people. A case study found that syrian phosphate industry was the main source of the radionuclides enhancement in the environment of Syria [*othman2007impact*].The most common methods for removing phosphate from aqueous solutions are chemical, physical, or biological ones. Although biological treatment is a very effective approach, it is expensive and susceptible to many other influences [*oehmen2007*]. Chemical precipitation is the most used method due to its low cost; however, it generates large amounts of sludge, which leads

to secondary pollution. Among these methods, adsorption technology is considered to be the most effective for removing phosphates at low concentration. It is also easy to operate and costing is low and the design is relatively simple and does not cause secondary pollution.

As a result, throughout the last decade, research has concentrated on high-capacity adsorbent as well as adsorbent regeneration conditions[*almanassra2020*]. Numerous adsorbents, including sludge [*song2011*], mesoporous material [*huang2017*], activated carbon [*ouakouak2016*], binary oxides [*lu2014phosphate*] and gas concrete [*oguz2003removal*], have been used to remove phosphate from aqueous solutions. Activated carbon is one of these adsorbents that has been utilized extensively for the removal of phosphates because of its high surface area, stability, and porous structure. Activated carbon often shows hydrophobic or weak charged group thus, it performs poor phosphate adsorption capacity. To enhance their ability to adsorb phosphate, metal ions were added to or impregnated into activated carbons [*yang2018,almanassra2020*]. Nevertheless, finding the less expensive adsorbents with more phosphate capacity is still ongoing research.

Countries		
	Surface water	**Ground water**
Nigeria	8.1 (Alboy River)	1.41 (Lagos)
Argentina	6.6 (Jocoli river)	0.509 (Abasto sur dairy basin)
Russia	0.025 (Tolych river)	-
Thailand	0.02(Dang river basin)	15.2 (Saraburi Province)
Bangladesh	26.1 (Turag river)	0.48 (Khulna)
Egypt	0.248(El sharqia)	0.295(El sharqia)
India		0.0446
China	0.44(Nanxi river)	2.12 (Ganfu plain, south china)
USA	0.52 (Ichu river)	-
Indonesia	1.37(Krukut river)	1.32(Gunpang village)
Brazil	-	2.32(Marica municipality)
Japan	0.2±0.1µM (Obama Bay)	5.6±10.9µM

Table 1: Phosphate concentrations in different countries around the world

2.1.1 Phosphate

Phosphate is an inorganic chemical compound containing the phosphate ion (PO_4^{3-}). Phosphorous (P) is a limiting nutrient in freshwater systems that even at low concentrations of 0.01 to 0.1 mg/ L P can cause excess algae growth and eutrophication, which damage water resources and harm aquatic flora and fauna, and human well-being. Phosphate is a form of phosphoric acid, which contains phosphorus. In the body, phosphates are found in the bones and teeth. Phosphates may be used to treat a high level of calcium in the blood. Adding or removing phosphate chemical groups may affect the way proteins act in the body. Phosphate (PO_4) is usually found as calcium phosphate in rock deposits known as apatite and it is a natural source of phosphorus, an element that is essential to l

Year	Global phosphate demand for fertilizers (million-ton P_2O_5)	Global phosphate demand for non-fertilizers (million-ton P_2O_5)	Global mines production of phosphate rocks (million ton)
2015	41.74	3.52	241
2016	41.95	3.57	255
2017	43.20	3.62	269
2018	44.12	3.65	270
2019	45.01	3.69	-
2020	45.13	3.73	-
2023/2024	49.60	-	-

Table 2: Global demand of phosphate fertilizer and mine production of phosphate rock

life on earth. Global demand of phosphate fertilizer and mine production of phosphate rock is described in the Table-2

Table 3: Permissible Limits of Phosphate

Contaminants	***EPA***	***GUIDELINES FOR DRINKING-WATERQUALITY*** **WHO (1999)**	***FEPA standard***
Phosphate (PO_4^{2-})	Inland surface water = 5 mg/l	Acceptable limit = 0.1 mg/l Permissible limit =1 mg/l	Waste water = 20 mg/l Surface water = 13.5 mg/l

2.1.2 Sources of Phosphate

A. Natural Source*:*

- Rocks and Minerals: Phosphates are primarily found in the form of phosphate minerals, such as apatite, in sedimentary rocks. These rocks undergo weathering processes, releasing phosphates into the soil and water.
- Soil: Weathering of phosphate-rich rocks gradually releases phosphates into the soil, where they become available to plants. Over geological time scales, erosion and sedimentation redistribute phosphates within the Earth's crust.
- Oceanic Deposits: Marine organisms incorporate phosphates into their skeletal structures, which accumulate on the ocean floor over time, forming phosphate-rich deposits.

B. **Anthropogenic sources:**

- Agricultural Activities: Phosphates are key components of fertilizers used to enhance soil fertility and crop yield. However, excessive fertilizer application can lead to the accumulation of phosphates in soil and runoff into water bodies, causing eutrophication.
- Industrial Processes: Phosphates are utilized in various industrial applications, including the production of detergents, food additives, metal surface treatments, and flame retardants. Industrial activities may release phosphates into the environment through wastewater discharge and air emissions.

- Wastewater: Human activities, such as domestic sewage, industrial effluents, and runoff from urban areas, contribute phosphates to wastewater. Inadequate wastewater treatment can result in the discharge of phosphates into rivers, lakes, and oceans, impacting aquatic ecosystems.

C. Biological sources:

Phosphates are essential nutrients for all living organisms. Plants absorb phosphates from the soil through their roots and incorporate them into various biomolecules, such as DNA, RNA. Animals obtain phosphates by consuming plants or other animals.

2.1.3 Effects of varying concentrations of phosphate on human health

- ***Phosphate toxicity on Human health***

Phosphate toxicity, also known as hyperphosphatemia, occurs when there is an excessive accumulation of phosphate in the blood. This condition can have various adverse effects on health, particularly when prolonged or severe.

Phosphate homeostasis involves several major organs that are the skeleton, the intestine, the kidney, and parathyroid glands. Major regulators of phosphate homeostasis are parathormone, fibroblast growth factor 23, 1,25-dihydroxyvitamin D, which respond to variations of serum phosphate levels and act to increase or decrease intestinal absorption and renal tubular reabsorption, through the modulation of expression of transcellular transporters at the intestinal and/or renal tubular level. Any acquired or genetic dysfunction in these major organs or regulators may induce hypo- or hyperphosphatemia. The causes of hypo- and hyperphosphatemia are numerous. Here are some of the potential consequences of phosphate toxicity:

- **Hyperparathyroidism:** Moderate hypophosphatemia, usually between 0.6 and 0.8 mmol/L, is reported in 50 to70% of patients with primary hyperparathyroidism.

- **Calcification of Soft Tissues**: Elevated phosphate levels can lead to the deposition of calcium-phosphate crystals in soft tissues throughout the body, a process known as ectopic calcification. This can affect organs such as the kidneys, heart, blood vessels, lungs, and skin, impairing their function and potentially leading to organ damage.

- **Cardiovascular Complications**: Hyperphosphatemia has been associated with an

increased risk of cardiovascular disease. Excessive phosphate levels can contribute to arterial calcification, atherosclerosis (hardening and narrowing of the arteries), and vascular stiffness, which may elevate blood pressure and increase the risk of heart attacks and strokes.

- **Mineral and Bone Disorders**: Chronic phosphate toxicity can disrupt the balance of minerals in the body, leading to mineral and bone disorders (MBD). High phosphate levels can stimulate the release of parathyroid hormone (PTH), which promotes the mobilization of calcium from bones to maintain normal blood calcium levels. This can weaken bones and increase the risk of fractures, osteoporosis, and other skeletal abnormalities.

- **Renal Impairment**: Hyperphosphatemia can exacerbate kidney disease and impair renal function. The kidneys play a crucial role in regulating phosphate levels in the blood by excreting excess phosphate through urine. In individuals with kidney dysfunction, impaired phosphate excretion can lead to further accumulation of phosphate in the bloodstream, worsening mineral and bone disorders and increasing the risk of cardiovascular complications.

- **Neurological Symptoms**: Severe phosphate toxicity may manifest with neurological symptoms such as confusion, weakness, seizures, and coma. These effects may occur due to disturbances in electrolyte balance, metabolic abnormalities, or direct effects of phosphate on neuronal function.

- **Metabolic Acidosis**: In some cases, hyperphosphatemia may contribute to metabolic acidosis, a condition characterized by an imbalance in the body's acid-base status. Excessive phosphate levels can disrupt pH balance by affecting the buffering capacity of bicarbonate ions in the blood, leading to acidosis.

- **Muscle Dysfunction**: High phosphate levels can interfere with muscle function and contribute to muscle weakness, cramping, and fatigue. Phosphate imbalances may disrupt cellular energy metabolism and impair the contractile properties of skeletal and cardiac muscle fibres

  Phosphate is an essential electrolyte in the human body as it constitutes about 1% of the total body weight. In an adult, the normal serum phosphate level ranges between 2.5 to 4.5 mg/d L. The normal serum levels of phosphate tend to decrease with age and its

highest levels i.e., 4.5 to 8.3 mg/dL are seen in infants, about 50% higher than adults; this is because infants and children need more phosphate for their growth and development.

Table 4: Different concentration of phosphates and their consequences

Normal serum phosphate in adults	2.5-4.5 mg/dL
Hypophosphatemia	2-2.5 mg/Dl or <1mg/dL
Hyperphosphatemia	>4.5 mg/dL

2.1.4 Magnitude of excess Phosphate contamination Problem

Excess phosphorus inputs to lakes usually come from industrial discharges, sewage and runoff from agriculture, construction sites, and urban areas. The input of P to soil creates the potential for an increase in transfer to the wider environment. Phosphorus sources can be natural which includes indigenous soil P and atmospheric deposition and/or anthropogenic which includes fertilizers, animal feed input to the farm and manure applied to the soil. In addition, ground water can potentially contribute significant amount of P in water bodies driving eutrophication process

2.1.5 Phosphate Mitigation strategy:

There is need to reduce anthropogenic nutrient inputs to aquatic ecosystems in order to reduce the negative effects of eutrophication. It has been indicated that reducing P input in the water bodies leads to eutrophication mitigation. Derived this conclusion from four methods, all long-term studies at ecosystem scales:

i. long-term case histories,

ii. multiyear whole lake experiments,

iii. experiments where chemical treatments are used to remove phosphorus from the water column, and

iv. chemical additions to inhibit return of phosphorus from the sediments to the water column.

However, argued that P based nutrient mitigation commonly regarded as the key tool in eutrophication, in many cases has not yet yielded the desired reductions in water

quality and nuisance algal growth in water bodies has not reduced in decades of reducing P input. argued that these observations could be as a result of:

i. legacies of past land-use management;

ii. decoupling of algal growth responses to river P loading in eutrophically impaired aquatic system; and

iii. recovery trajectories, which may be nonlinear and characterized by thresholds and alternative stable states.

Therefore, as a result of these contrasting findings there is need in some cases to consider a combination of different P mitigation strategies for example employing control of nutrient loading, physicochemical and physico-mechanical method simultaneously. Control or mitigation of P eutrophication should encompass multiple components which could include; control of pollutant sources, restoration of the damaged ecosystem, and catchment management

CHAPTER-2

3.1 LITERATURE REVIEW:

3.1.1 Literature Review

Sl No	Title of research	Year of Publication	Material used	Methodology	Major findings
1	A novel magnetic biochar efficiently sorbs organic pollutants and phosphate	2010	The magnetic biochar was prepared with orange peel as the raw biomass material and magnetite	Elemental characterization and sorption study	The magnetic biochars exhibited a hybrid sorption property to effectively remove organic pollutants and phosphate simultaneously
2	A novel magnetic biochar efficiently sorbs organic pollutants and phosphate	2011	Magnetic biochar was prepared with orange peel as the raw bio mass material and magnetite as the objective magnetic medium by a method of chemical co precipitation and subsequently pyrolyzing under different temperature	Batch study and adsorption isotherm	Removal efficiency of magnetic biochar (except MOP400) was much higher
3	Adsorption of Phosphate by Biomass Char Deriving from Fast Pyrolysis of Biomass Waste	2012	The raw biomass material was pine sawdust	Adsorption kinetics, isotherm and thermodynamics study	Phosphate adsorption by biomass char (BC) from fast pyrolysis, finding adsorption capacity dependent on pyrolysis conditions. maximum adsorption capacity for phosphate was approx 15.11mg/g

4	Modification and use of biochar from wheat straw (Triticium aestivum) for nitrate and phosphate removal from water	2014	Biochars were produced from wheat straw through low-temperature pyrolysis at approximately 450°C, activated with hydrochloric acid (HCL) and coated with iron ($FeCl_3$. $6H_2O$) of different amounts	Batch study Absorption and kinetic study	Adsorption capacity was calculated based on the amount of pure nitrogen or phosphorus. The maximum adsorption capacities were 2.47 and 16.58 $mg.g^{-1}$
5	Kinetic study on phosphate removal from aqueous solution by biochar derived from peanut shell as renewable adsorptive media	2015	Biochar derived from oak and bamboo woods, Maize residue, soybean stover, and peanut shells	Kinetic study and Adsorption test	Peanut shells (PSB), demonstrates superior phosphate removal compared to traditional adsorptive media. PSB exhibited the highest phosphate removal rate at 61.3%
6	Modification and use of biochar from wheat straw (Triticum aestivum L.) for nitrate and phosphate removal from water	2016	Wheat straw	-	Surface modification of wheat straw-derived biochar with hydrochloric acid (HCl) activation and iron ($FeCl_3$,$6H_2O$) coating significantly enhances adsorption capacity. Optimal iron-to-biochar ratio for coated biochar is 0.70.
7	Adsorption and desorption of phosphate on biochars	2016	sugar cane bagasse (SC) and of Miscanthus giganteus (M).	Adsorption and desorption study	Carbonized sugar cane bagasse (SC) and Miscanthus giganteus (M) biochars show promising phosphate adsorption capacities, influenced by carbonization temperature and residence time. M

					biochar, carbonized at 700°C with longer residence time, exhibits superior phosphate adsorption
8	Removal of nitrate, ammonia and phosphate from aqueous solutions in packed bed filter using biochar augmented sand media	2017	Eucalyptus woody biomass	Laboratory investigation of the efficiency of packed bed filters to remove nitrate, ammonium and phosphate from aqueous solutions were conducted. Sand and Sand augmented with hydrochloric acid treated biochar (SBC) were used as packing media.	Over the experiment period, the average removal efficiency of $(PO_4)_3^-$, NO_3^-, NH_4^+ were 99.2%, 72.9%, 96.7% in the sand packed columns and 99.2%, 82.3%, 97.4% in the sand packed columns respectively
9	Biochar from green waste for phosphate removal with subsequent disposal	2017	Cotton stalks	Adsorption isotherm and soil microbial fuel construction	The study explored cotton stalk biochar (CSB) as an effective adsorbent for phosphate removal. CSB also showed potential as a nutrient enhancer for plant growth and microbial population multiplier in MFCs
10	Removal and recovery of phosphate from water by Mg-laden biochar. Batch and column studies	2018	Mg-laden biochar prepared from Mg-enriched bamboo to remove and recover phosphate	Batch and column studies	Removal efficiency of phosphate is 90%
11	Biochar	2018	B. papyrifera leaves	Adsorption	Broussonetia

	synthesized via pyrolysis of Broussonetia papyrifera leaves: mechanisms and potential applications for phosphate removal			kinetics and isotherm studies	papyrifera leaves biochar effectively adsorbed phosphate from water, with enhanced adsorption under alkaline conditions
12	Engineered/designer biochar for the removal of phosphate in water and wastewater	2018	Iron oxide, Zeolite, Montmorillonite		This review focuses on recent advancements in biochar technology, especially with respect to its technical aspects, the variables associated with removing phosphates from water, and the challenges for such abatement
13	Phosphorus removal from eutrophic water using modified biochar	2018	Poultry manure (PM), collected at a farm and sugarcane straw (CS) from a sugar/ethanol production site	Adsorption and TGA analysis	Biochar derived from poultry manure (BPM) and sugarcane straw (BCS), post-doped with aluminum, exhibits high maximum phosphorus adsorption capacities (MPAC) of up to 758.96 mg/g. Fragmented materials retain slightly lower MPAC values but still demonstrate significant adsorption capabilities
14	A green approach for iron removal and subsequent phosphate	2019	Four parts of palm wastes, palm coir, palm leaf lets, date empty bunches and date stone were	Batch and column study and adsorption mechanism	Removal efficiency groundwater-86.64% Synthetic water 94.10%

	removal in Al Khagra (Egypt) using date palm biochar and its usability: case study		used to prepare biocha		
15	Adsorption of phosphate from aqueous solution by vegetable biochar/layered double oxides: Fast removal and mechanistic studies	2019	The original Chinese cabbage and rape. Leaves and stems are used	Batch adsorption study	The biochar/LDOs showed high phosphate removal efficiency (>92%) across a wide pH range, rapid adsorption kinetics, and were well described by kinetic and isotherm models.
16	Preferable phosphate removal by nano-La(III) hydroxides modified mesoporous rice husk biochars: Role of the host pore structure and point of zero charge	2019	rice husks were collected from Honghu	Batch study	The study focused on La-modified rice husk biochars (RHBCs) for phosphate adsorption, emphasizing pore structure and pHpzc effect. Higher mesoporous rates in RHBCs led to faster adsorption.
17	Removal efficiencies of manganese and iron using pristine and phosphoric acid pretreated biochar made from banana peel	2020	Pristine banana peel biochar (BPB) and phosphoric acid pretreated biochars (PBPB) derived from banana peels	Batch study and absorption isotherm models	Removal efficiency of Fe by PBPB = Fe by 96%, removal efficiency of Fe by BPB = 85% Removal efficiency of Mn by BPB = 32% and 46% by PBPB
18	Comparative adsorptive removal of phosphate and nitrate from wastewater using biochar-MgAl LDH	2020	Date palm biochar MgAl- augmented double layered hydroxide	Batch study Adsorption and kinetic study	The maximum monolayer adsorption capacities of phosphate and nitrate by the nonlinear langmuir model were 177.97

	nanocomposites: coexisting anions effect mechanistics studies				mg/g and 28.06 mg/g at 308 and 298 K respectively
19	Characteristics and mechanism of phosphorous adsorption by rape straw derived biochar functionalized with calcium from eggshell	2020	Rape straw and modified with eggshell	Kinetic and isotherm analysis	ERS and CRS show distinct adsorption performance for the phosphate removal with the equilibrium adsorption amounts of 109.7 mg/g and 101.0 mg/g respectively
20	Efficiency of iron and calcium impregnated biochar in adsorbing phosphate from waste water in on site wastewater treatment systems	2020	Potential of biochar impregnated with Fe^{3+} or Ca^{2+} or mixed with polonite as a filter material for removal of phosphate from wastewater in onsite wastewater treatment system	Batch and column studies	Biochar impregnated with $FeCl_3$ work best for the removal
21	Adsorption removal and reuse of phosphate from wastewater using a novel adsorbent of lanthanum-modified platanus biochar	2020	Lanthanum nitrate hexahydrate (La(NO3)3·6H2O), anus balls	Batch adsorption and Fixed bed columns	La-TC, a novel lanthanum-modified platanus ball fiber biochar, exhibited a high phosphate adsorption capacity of 148.11 mg/g under specific conditions
22	Phosphogypsum as a novel modifier for distillers grains biochar removal of phosphate from water	2020	Distillers grains were sampled from a local distillery, Phosphogypsum was collected from a phosphate fertilizer plant.	Adsorption isotherm and kinetic study	Biochar composite, synthesized from distillers' grains-treated phosphogypsum, demonstrates superior phosphate adsorption capabilities. The composite exhibits a

					maximum phosphate adsorption capacity of 102.4 mg/g, significantly higher than distillers grains biochar alone (21.5 mg/g).
23	Mechanism of phosphate removal from aqueous solutions by biochar supported nanoscale zero-valent iron†	2020	Rape straw	Batch adsorption, isotherm and kinetic study	The study investigated phosphate removal mechanisms using rape straw biochar (RSBC) supported nanoscale zero-valent iron (nZVI)
24	A comparative study on phosphate removal from water using Phragmites australis biochars loaded with different metal oxides	2021	Five biochars loaded with Al, Ca, Fe, La and Mg oxides respectively using Phragmites	Batch study Absorption isotherm	Mg-BC is suggested for phosphate removal from water considering both phosphate adsorption rate and capacity
25	The potential of date palm waste biochar for single and simultaneous removal of ammonium and phosphate from aqueous solutions	2021	Date palm fronds and leaves waste	Adsorption isotherm, kinetic study and fixed bed column study	Date palm waste biochar effectively removed NH4+ and PO43- ions from aqueous solutions
26	Fe-loaded biochar obtained from food waste for enhanced phosphate adsorption and its adsorption mechanism study via	2021	Food waste and Fe	Batch study	The study optimized Fe-loaded food waste biochar (Fe-FWB) production using response surface methodology, finding favorable conditions for phosphate removal.

	spectroscopic and experimental approach				Pseudo-second order and Elovich models described kinetics, while Freundlich and Redlich–Peterson isotherms better simulated adsorption.
27	Preparation and application of novel rice husk biochar calcitecomposites for phosphate removal from aqueous medium	2021	Rice Husk and Calcite	Adsorption isotherm and Kinetic study	The maximum removal and adsorption capacities of optimized BRH-C were 87.3% and 1.76 mg/g, respectively, at low phosphate concentrations. The pyrolysis temperature had positive linear and quadratic effects on the phosphate removal, whereas the pyrolysis time had a negative quadratic effect.
28	A state of the art review on phosphate removal from water by biochars	2021			Unmodified BCs exhibit limited phosphate sorption capacity, but engineered BCs, especially those decorated with elements like magnesium, aluminum, calcium, lanthanum, and iron, show significantly enhanced adsorption capabilities.
29	Competitive or synergetic? Adsorption mechanism of phosphate and oxytetracycline on chestnut shell-derived	2022	KH_2PO_4, Chestnut shell		Modified biochar (MBCCS) with Fe and Mn ions showed high adsorption capacities for phosphate and oxytetracycline

	biochar				
30	Simultaneous adsorption of phosphate and tetracycline by calcium modified corn stover biochar: Performance and mechanism	2022	Ready-made corn stover powder		The maximum adsorption capacities of phosphate and tetracycline were 33.94 and 33.53 mg/g respectively
31	Removal of phosphate by a novel activated sewage sludge biochar: Equilibrium, kinetic and mechanism studies	2022	The raw sewage sludge (RS) used came from the condensing tank from wastewater treatment plant without any digestion treatment	Batch study, Kinetic and equilibrium study	Mg-SB, a novel biochar adsorbent modified with magnesium oxide particles, demonstrates exceptional phosphate removal performance, achieving a maximum capacity of 97,450 mg/kg PO_4^{3-}. This exceeds capacities reported for other adsorbents.
32	Feasible synthesis of a novel and low-cost seawater-modified biochar and its potential application in phosphate removal/recovery from wastewater	2022	Fir wood waste was obtained locally and sea water collected from Sansha bay	Batch and column study	seawater-modified biochar (SBC) via firwood waste pyrolysis and co-precipitation, exhibited high phosphate adsorption capacity (181.07 mg/g)
33	Concentration-dependent adsorption behaviors and mechanisms for ammonium and phosphate removal by optimized Mg-impregnated biochar	2022	Crushed rice straws, $MgCl_2$	Isotherm and Kinetic study	Mg-impregnated biochar for simultaneous recovery of ammonium and phosphate, achieving high Langmuir adsorption capacities (5.5 mmol/g for

					ammonium, 4.4 mmol/g for phosphate)
34	Removal of phosphate from water by paper mill sludge biochar	2022	Paper mill sludge obtained from waste water treatment plant of paper	Adsorption kinetics, Isotherm and batch study	paper mill sludge into metal/metal oxide-embedded biochar (PMSB) via pyrolysis, enhancing phosphate (P) removal. PMSBs showed adsorption capacities ranging from 9.75 to 25.19 mg P/g
35	Production and characterizatio n of porous magnetic biochar: before and after phosphate adsorption insights	2022	Biochars were produced from spruce sawdust	Adsorption and desorption study, Batch study	PMB showed high phosphate removal (100% at 5 mg/L P), with optimal performance observed for biochar produced at 200/800 °C (30% removal at 25 mg/L P)
36	Recovery of phosphate from aqueous solution by dewatered dry sludge biochar and its feasibility in fertilizer use	2022	Dewatered dry sludge with moisture of ~39% was collected from a sewage treatment plant	Batch adsorption and desorption study	At 700°C, biochar contained CaO and MgO, enhancing phosphate adsorption. Adsorption increased with pH. Kinetics followed pseudo-second-order, with a maximum adsorption capacity of 51.79 mg/g according to Langmuir isotherm
37	Selective adsorption behaviour and mechanism of phosphate in water by different lanthanum modified biochar	2022	Wheat stalks	Characterizati on and adsorption study	The study compared lanthanum carbonate/biochar (LCB300) and lanthanum hydroxide/biochar (LHB800) composites for phosphate (P) adsorption selectivity. Both exhibited similar

					maximum adsorption capacities (64.3 and 65.0 mg/g, respectively), but LHB800 showed higher selectivity (90–100%)
38	Utilization of activated sludge and shell wastes for the preparation of Ca-loaded biochar for phosphate removal and recovery	2023	egg shells and oyster shells were collected from kitchen garbage.	Batch adsorption, Isotherm, Leaching and Kinetic study	Egg shell-modified activated sludge biochar (ESB) and oyster shell-modified activated sludge biochar (OSB) loaded with calcium (Ca) exhibit promising phosphate adsorption capacities. ESB demonstrates superior performance, with a maximum adsorption capacity of 154.18 mg/g compared to OSB's 129.03 mg/g.
39	Preparation of iron/calcium-modified biochar for phosphate removal from industrial wastewater	2023	Agricultural and forestry wastes from bamboo, wheat bran, bagasse, and poplar wood	Kinetic study and Synergistic removal study	Fe/Ca-modified biochar, particularly iron/calcium oxide-modified bamboo biochar (ZFCO-BC), exhibits significantly enhanced phosphate adsorption capacities, up to 70 times higher than unmodified biochar. ZFCO-BC effectively removes phosphate from high-concentration wastewater, forming stable vivianite.
40	Removal and recovery of phosphate from water by	2023	Moso bamboo (Phyllostachys pubescens) more than 3 years old	Batch and Column study	Mg-laden biochar derived from Mg-enriched bamboo demonstrates

	Mg-laden biochar: Batch and column studies		was selected as biomass feedstock		excellent potential for phosphate removal and recovery from water. The maximum phosphate adsorption amount was 370 mg/g for biochar Mg-600

3.1.2 Research Gap:

From the literature review, few/no researches are there on the adsorption studies of phosphate, nitrate, iron, fluoride using jute biochar. From there following research gaps are noted.

- Application of a new form of jute biochar in the removal technology.
- Application of jute biochar for phosphate removal is very few.
- To use the jute biochar in the removal process of phosphate, nitrate, fluoride and iron. (modification if required)
- To check the effect of different structural and textural characteristics of the available jute biochar in contaminant removal.
- To check the applicability of the jute biochar sludge after contaminant removal to enhance soil fertility.

CHAPTER-3

4.1 OBJECTIVE & SCOPE OF WORK

4.1.1 Objective of the study:

- To study the feasibility of jute biochar as a substitute for the conventional, commercially available costly adsorbent used for removing pollutants from ground water. The study can be done using optimization processes like batch study and column study.
- To determine the reusability of the biochar for achieving an economical and environmentally sustainable process.
- Recovery of raw materials from the used adsorbent. To reduce the release of pollutant in water body, and to make the process more economical by utilizing that component again.
- To check the functional group responsible for removal using FTIR and other surface characteristics like FESEM, TGA, BET, FTIR and XRD analysis.

4.1.2 Scope of the study:

The scope of the present studies are:

1. To identify the phosphate-affected zone.
2. To observe the phosphate concentration in ground and surface water in affected areas.
3. Phosphate removal capacity of the locally available jute fibres.
4. Comparative study of phosphate removal efficiency of Jute fibres.
5. Cost analysis of the filter developed as a mitigation strategy.

CHAPTER-4

5.1 BIOCHAR

Bio-char is a pyrogenic black carbon solid that is produced by thermochemically converting carbon rich biomass at different temperatures while limited amount of oxygen is present [*qiu2021*]. Recently, biochar has drawn more attention due to its multi-functional use such as soil fertility enhancement [*yadav2016vacuum*] and production of bio energy. Although biochar is primarily used as a soil supplement, it also used as an inexpensive wastewater treatment method because of its adsorption properties. Though activated carbon is already utilised for this purpose, biochar could serve as a more affordable substitute [*patra2017*]. A pyrolytic byproduct of the synthesis of bio-oil is bio-char [*mohan2007*]. Biochar has a complex micro structure with many pore spaces, which helps to increase its specific surface area because of its abundant sources of carbon. The surface area of biochar usually ranges from 100 to 460 m^2g^{-1}, and it contains a variety of functional groups, such as hydroxyl, carboxylic, phenolic, and carbonyl groups [*haider2022*]. Higher lignin concentrations in biomass result in higher yields of biochar, but higher cellulose or hemicellulose contents led to easier thermal or chemical alterations to create functional groups [*gupta2020*]. Biochar contains metal elements mostly come from two sources. The first is the soil's absorption of various mineral components (such as calcium, iron, magnesium, aluminum, and potassium) during the growth of raw biomass. The other source is artificially added metal salts that are



Fig 2: Biochar made from Jute fibre

added during the pretreatment process. These multipurpose qualities provide biochar a good potential for application as an efficient environmental adsorbent for the removal of NH_4^+, PO_4^{3-} etc from water [*yin2017biochar*]. According to literatures, biochar adsorbents' surface area increased between 300°C and 400°C in the majority of situations [*mohan2007,srivastav2021*]. It might also be influenced by the raw materials used to make biochar. Furthermore, energy consumption will increase proportionately with temperature. More energy is needed if the biochar matrix is modified [*srivastav2021*]. Production of biochar has many ways such as slow pyrolysis, gasification, fast pyrolysis and hydrothermal processing [*lehmann2015*]. Different types of biochar are used e.g. modified, animal or plant based, for the removal of phosphate in aqueous solution. For instance, Double hydroxide biochar [*wan2017*], Date palm waste biochar [*fseha*], zeolite biochar [*deng2022removal*], and MgO modified magnetic biochar [*liu2019removal*] are few types of biochar which are used to remove phosphate.

The current work offers a thorough and critical analysis of the literature on the adsorptive removal of phosphate in aqueous solution with the help of plants, agricultural wastes and modifications of biochar. A summary of published data in terms of adsorption mechanism, adsorption thermodynamics, maximum adsorption capacity, characterization and removal efficiency and bibliometric analysis are presented. In addition, future directions for phosphate removal with the help of biochar are also emphasized.

5.1.1 Application of biochar in phosphate removal

A life cycle study of pyrolysis-biochar systems revealed that, while heat pyrolysis can turn practically any biomass into biochar, producing biochar from waste biomass is more economically and environmentally sustainable. Still, the feedstock, processing, and ambient conditions all affect how stable the biochar is [*roberts2010life*]. Agricultural wastes, such as sugarcane bagasse, poultry litter, and manure, together with other green waste, have been suggested as suitable feedstock materials for the production of biochar.

As far as the environment is concerned, biochar made from a variety of wastes helps to lessen environmental burdens and once phosphate has been removed, are effectively used for soil remediation [*almanassra2020*]. Being mindful of the environment, three distinct areas in this literature demonstrate the use of biochar to remove phosphate from water: Plant or animal-based, Agricultural waste-based, and Modified biochar.

5.2 Plant/Animal based adsorbent:

The use of biochar derived from plant or animal waste is growing these days since it is an affordable, removal efficiency of phosphate is good and efficient method of recycling waste materials. In this literature, different kind of plants or animal which are used to make biochar and helped to remove phosphates are compiled in a Table 2. In spite of the wastes from animals and plants, some plants are harmful for nature itself. For instance, invasive plants are the harmful plants for environment, natural habitat and human health because of their rapid spreading ability, in China, it's even ranked as the most damaging plant. Therefore it is good to use this kind of plants as a biochar. But the removal efficiency of phosphate using plant or animal waste based biochar is quite high. For example, Mg-biochar from ground coffee waste absorbed around 89% of phosphate in aqueous solution [*shin2020*]. Some of the plant based biochar exhibited 100% removal efficiency of phosphate for instance, in modified paulownia biochar, the greatest phosphate removal effectiveness at a concentration of 14 mg/L was 100%. Various animal species' manures also pyrolyzed to produce an alkaline biochar that is mostly stable and aromatic carbon structures.

5.3 Agricultural waste-based adsorbent:

A sustainable and affordable supply of adsorbents for the removal of phosphates from water is agricultural waste. Pollution of the environment is being caused by agricultural wastes. Reusing agricultural trash to create biochar is a workable and useful way to increase the amount of waste that agriculture produces. For example, the agricultural output that has contributed to environmental

contamination in recent decades is straw waste [*yuan2021facile,huang2020modified*]. Hence, it is a good practice to reuse such kind of wastes as a biomass based adsorbent to remove phosphates in aqueous solution. Another illustration includes, cash crop waste, an agricultural waste, causes economical and environmental problem. Recycling the cash crop waste as a biochar could lessen its negative effects on the environment [*salimova2020*].

5.4 Phosphate removal from water using modified biochar:

According to certain research, it has been discovered that while pure biochar has limited functionality in terms of its ability to adsorb phosphate, biochar treated chemically with cationic substances (such as Fe, Mg, Al, or Ca) can significantly increase the adsorption of phosphates [*deng2021*,*yin2018*]. Because of their net negative surface charge, the majority of biochar forms have a low attraction for anions like phosphate. For example, adding iron to the surface of biochar can raise its positive surface charge, which improves the material's ability to exchange anions and improves its redox characteristics [*ou2023*]. Plant based biochar is economical and environment friendly even the adsorption capacity is also good but if it is modified with other substance then the adsorption capacity will become more. For instance, maximum adsorption capacity of platanus biochar was 55.56 mg/g whereas the lanthanum modified platanus biochar showed high adsorption capacity of phosphate, 148 mg/g [*jia2020*].

Table 4 provides information about the removal and adsorption capacity of phosphate in aqueous solution using modified biochar.

Adsorbent	Modification/ Activation agent	BET surface area(m2/g)	Adsorbent dose (g/L)	Studied phosphate concentration	Pyrolysis temperature /Residence time	Optimum pH	Adsorption capacity %	Phosphate removal efficiency	zeta potential	PZC	Adsorption capacity, qm (mg/g)	Enthalpy kJ/mol	Gibbs free Energy kJ/mol	Modification/Pyrolysis method	Isotherm	Reference	Year
Sugar beet tailing	Ferric hydroxide(Fe-STC)	351 (CO_2) 2.6 (N_2)	0.1 g	50mL	600C/2hr	9.45	8%		-54.23 mV		Nil	Nil	Nil	Cylinder reactor furnance	Nil	Yao et.al 2011	2011
Digested sugar beet tailing	Ferric hydroxide(Fe-DSTC)	449 (CO_2) 336 (N_2)	0.1 g			9.95	22%	73%	-18.11 mV								
Peanut shell	Nil	328.96	1.0g	1-50mg/L	700C/3hr	10.01	61.30%	>50%	-16mV	Nil	Nil	Nil	Nil	Muffle furnance	L,F	Zung et.al 2015	2015
Date Palm	Nil	Nil	0.05-0.4g	Nil	500C, 600C	7	Nil	51.53 % (Single soln) 52.42 % (mixed)	Nil	6-8	26.90mg/g 27.41mg/g	Nil	Nil	Batch and fixed bed column study	L.F	Fseha et.al 2021	2021
Ground coffee bean	$MgCl_2$	36.4	0.2g	Nil	500C/50 min	4,7		89.40 %		Nil	63.5mg/g	Nil	Nil	Pyrolyzer with N2 gas	L,F,L-F,Temkin,Redlich-Peterson	Shin et.al 2020	2020
Phytoremediation plant	Nil	17.53(N2) 287.95(CO2)	0.2g	Nil	500 C(N_2)/2hr 700C(CO_2)/2hr	10.49	Nil	38.12 %	Nil	Nil	2.86mg/g	Nil	Nil	Furnance	L, F	Zheng et.al 2013	2013
Broussonet	Nil	9.53	0.1g	Nil	500C/2hr	Nil	Nil	Nil	(+-	Nil	28.20m	Nil	Nil	Muffle	F (25C),	Qui	20

ia papiryfera bc									)10 and (+-)30		g/g			furnance	L(35C), Temkin	et.al 2019	19
Orange peel bc	Ferrous and Ferric chloride	23.4	Nil	Nil	700C/6hr	Nil	Nil	9.3(+-)1.6%	Nil	Nil	2.4mg/g	Nil	Nil	Ceramic pot, Co-precipitation	L, F	Chen et.al 2010	2010
Pine sawdust bc	Nil	126 219	0.1g	10-60mg/L	823K/15 min 1023K/30 min	Nil	Nil	Nil	Nil	Nil	15.11mg/g	13.41	-6.49	Quartz tube reactor, electric furnance	L, F	Peng et.al 2012	2012
Eggshell biochar	Ca modified	34.84	0.05g	10-800mg/L	800C/2hr	12.9	Nil	Nil	Nil	8.9	106.99 mg/g	1.81	-2.41 to -3.03	Tube furnance, Co-pyrolysis	L,F	Yang et.al 2021	2021
Phragmites Australis bc	(Al,Ca,Fe,La,Mg) chlorides	89.82	2g	100-1500 mg/L	600C/2hr	Nil	Nil	Nil	Nil	11.3	104.6mg/g	Nil	Nil	Tube furnance	Nil	Wang et.al 2021	2021
Tomato tissues bc	Mg enriched	Nil	Nil	Nil	600C/1hr	Nil	Nil	88.50 %	Nil	>12	Nil	Nil	Nil	Tube furnance	Nil	Yao et.al 2013	2013
Sheep manure bc	Oyster shells	2.26	0.05g	Nil	500C/2hr	3-11	94%	Nil	Nil	Nil	146.3	Nil	Nil	Nil	L,F, Sips	Feng et.al 2021	2021

Table 5: Plant/Animal based adsorbent

Adsorbent	**Modification/ Activation agent**	**BET surface area(m2/g)**	**Adsorbent dose (g/L)**	**Studied phosphate concentration**	**Pyrolysis temp/Residence time**	**Optimum pH**	**Adsorption capacity, q_m (mg/g)**	**Adsorption capacity %**	**Removal capacity %**	**zeta potential mV**	**PZC**	**Gibbs free energy of adsorption kJ/mol**	**Enthalpy kJ/mol**	**Modification/ Pyrolysis method**	**Isotherm**	**Reference**	**Year**
Cotton stalk	Nil	Nil	1.0	15-50mg/l	450	7	Nil	Nil	Nil	Nil	Nil	-20 to -40	Nil	Nil	F, Temkin	Veni et.al	2017

Sugar cane bagasse Miscanthus	Nil	131 244	0.2	Nil	700C/1hr	4-10	13.21 16.10	Nil	Nil	28.4 to 34.9 -26.6 to -36.3	Nil	6.242 5.861	9.197 9.50	Electric furnance heater	L,F	Trazzi et.al	2015
Rice husk	Calcite	67.02	0.025-0.325	25-125mg/l	700C/2.3hr	9.5	1.76	Nil	87.30 %	Nil	Nil	Nil	Nil	Tube furnance	L,F	Ramola et.al	2021
Corn stover BC	CaCl2	238.30cm2/g	1.0	10-100	800C/1hr	6	33.94	50.86%	85.90 %	Nil	Nil	Nil	Nil	Tube furnance	L,F	Zhuo et.al	2022
Chinese cabbage	(Mg and Al) nitrate	124	0.05	Nil	500C/2hr	Nil	127.23		>92%	9.54	Nil	Nil	Nil	Muffle furnance	L,F		2019

Table 6: Agricultural waste-based adsorbent

Adsorbent	**Modification/Activatiion agent**	**BET specific surface area (m^2/g)**	**Adsorbent dose(g/L)**	**Studied phosphate concentration**	**Pyrolysis temperature /Residence time**	**Optimum pH**	**Adsorption capacity %**	**zeta potential**	**Adsorption capacity, qm (mg/g)**	**PZC**	**Phosphate Removal efficiency**	**Enthalpy kJ/mol**	**Gibbs free Energy (kJ/mol)**	**Pyrolysis/Modification method**	**Isotherm**	**Reference**	**Year**
Distillers grains bc	Phosphogypsum	Nil	0.05	5-500mg/L	600C	6	Nil	Nil	102.4	7.74	96.70%	Nil	-7.813 to -9.381	Nil	L	wang et.al	2020
Zinc oxide betaine modified bc	Ammonium zinc carbonate,AZnC	100.01	3	10-500mg/L	Nil	7	Nil	Nil	77.91	6.76	80%	Nil	Nil	Nil	L,F,T, D-R	Nakarmi et.al	2020
Magnetically modified BC	Ferric sulphate [$Fe_2(SO_4)_3$]	50.7 (wood)	Nil	25-150mg/L	600C/2hr	8.7	Nil	Nil	11.05	Nil	Nil	71.9	-5.379 to -9.140	Suspension	L,F	Ajmal et.al	2019

		3.72 (Rice husk)				7.1			9.38			31.5					
wheat straw chitosan bc	Chitosan with glutaraldehyde and Lanthanam hydroxide	Nil	Nil	Nil	550C/2hr 25min	5	93.00%	Nil	109+-4	Nil	Nil	Nil	Nil	Nil	L,F	Huang et.al	2019
$MgFe_2O_4$ bc	lanthanum alginate beads	181.8	0.6	5-50mg/L	600C/2hr	2-12	Nil	Nil	26.83	4.6	Nil	Nil	Nil	Co-precipitation	L,F,Temkin	Wang et.al	2019
Sea water modified BC	Sea water as Ca/Mg source	Nil	0.25-0.50	100mg/L	600C/2hr	10.5	Nil	Nil	181.07	11	Nil	Nil	Nil	Co-precipitation	L,F	Zhang et.al	2022
Activated sludge bc	FeCl3.6H2O	254.4	0.1	5-1000mg/L	550C/2hr	2-9	>60%	Nil	111	Nil	74.1-88.5%	Nil	Nil	Co-precipitation	L,F	Yang et.al	2017
Oak chips bc	Lanthanum nitrate[$La(NO_3)_3$]	45.79	0.1	1-400mg/L	500C	11.08	Nil	-5.1mV	46.37	Nil	Nil	Nil	Nil	Muffle furnance		Wang et.al	2016
Urban sewage sludge	Dolomite modified	11.31	2.6	Nil	800C/2hr	4.5	Nil	Nil	29.18	4.93	96.80%	Nil	Nil	Tube furnance	L,F	Li et.al	2019
Food waste bc	$FeCl_3$	10.42	Nil	Nil	600C/4hr	7	Nil	Nil	31.8	Nil	Nil	52.33	2.3 to 5.60		L,F, Redlich-Peterson		2021
Paper mill sludge bc	Nil	95.16	0.01-0.04g	20mg P/L	800C/1hr	Nil	Nil	Nil	25.19	Nil	Nil	85.33	-29.484 to -37.44	Nil	L	Zhang et.al	2021
Bamboo biomass	Polyethyleneimine polymer	2.634		20mg/L	600C/2hr	3			9.25+-0.4					Tubular furnace	L,F		2019

Table 7: Modified biochars for phosphate removal

CHAPTER- 5

6.1 MATERIAL & METHODS

6.1.1 Jute fibre collection:

The jute fibers were primarily collected from Calcutta Jute Mill. Total 1kg of jute samples are collected from the jute mill.



(a)



(b)

Fig. 3: Jute Fibres of size 2 to 4 mm

6.1.2 Preparation of biochar from jute:

The jute fibres are chopped into 2 to 4 mm size at first. After that chopped fibres were grinded in a mixer grinder and the sizes became less than 1 mm. After grinding the jute fibres, it is then drying in an oven for 72hrs for removing the moisture from the fibres.

6.1.3 Production of Biochar:

This section summarises several different carbonization processes to produce biochar along with their characteristics.

Pyrolysis:

Pyrolysis is a process for decomposing organic materials thermally under oxygen-free conditions in the temperature range, 300–900°C[20,21]. During thermal decomposition, cellulose, hemicellulose and lignin that comprise biomass undergo their own reaction pathways, including cross-linking, depolymerization and fragmentation at their own temperature, producing solid, liquid and gaseous products. The solid and liquid products are referred to as char and bio-oil, respectively, whereas the gaseous mixture containing CO, CO_2, H_2, and C_1–C_2 hydrocarbons are called syngas. The yields of the pyrolysis products depend on the characteristics of the raw biomass materials and the pyrolysis processes adapted. The parameters that influence the products of the pyrolysis processes include the reaction temperature, heating rate, and residence time. In general, the biochar yield decreases and the syngas yield increases with increasing pyrolysis temperature[22-24]. *Mohammad et al*. and *Zhang et al*. reported that the yields of biochar and acidic functional groups decreased with increasing pyrolysis temperature, whereas those of the basic functional groups, ash content, pH, and carbon stability increased. The increase in pH with increasing pyrolysis temperature was attributed to the reduction of organic functional groups, such as –COOH and –OH. The bio-oil yield was reportedly highest at approximately 500°C because cracking takes place at higher temperatures. Fig. 1 shows the elemental compositions of biochar produced at different pyrolysis temperatures. Pyrolysis processes are divided into slow pyrolysis and fast pyrolysis depending on the rate of the increase in temperature. In a slow pyrolysis, in which the pyrolyzed vapours reside for a long time in the reactor at low temperatures, continuing vapour-phase reactions increase the char yield. *Inguanzo et al*. evaluated the characteristics of the chars produced at two different temperature rising rates of 5°C/min and 60°C/min. They reported that the char produced at the higher temperature rising rate had a lower volatile matter content and a higher ash (including fixed carbon) yield and concluded that a high temperature rising rate is preferable in terms of the quality of the product biochar. This effect of the temperature rising rate was not observed at high pyrolysis temperatures. Therefore, fast pyrolysis is generally aimed at producing a liquid product at high yield. To suppress the gas production due to secondary cracking, the vapor residence time is controlled short and rapid cooling is used to maximise the liquid product yield. Regarding the effects of the residence time on the product composition in a pyrolysis process, *Zhang et al*. reported that the biochar yield decreased with increasing residence time at the same pyrolysis temperature. In a study of the effects of the residence time on the specific surface area and pore characteristics of biochar, *Lu et al*. reported that the specific surface area and pore area increased with increasing

residence time up to 2 h at 500–900°C but they decreased when the residence time exceeded 2 h. In particular, the specific surface area and pore area decreased rapidly when the residence time exceeded 2 h at high temperatures. *Bandosz et al.* observed in a study of the pyrolysis of sewage sludge that the specific surface area decreased from 141 m^2/g to 125 m^2/g and the pore volume decreased from 0.209 cm^3/g to 0.187 cm^3/g when the residence time was increased from 30 min to 1 h at a pyrolysis temperature of 950°C. *Lu et al.* attributed the results of *Bandosz et al.* to a narrowing and closure of the pore entrances owing to the sintering of char, resulting in a reduction of the specific surface area. Table 1 summarises the characteristics of biochar produced under various pyrolysis conditions.

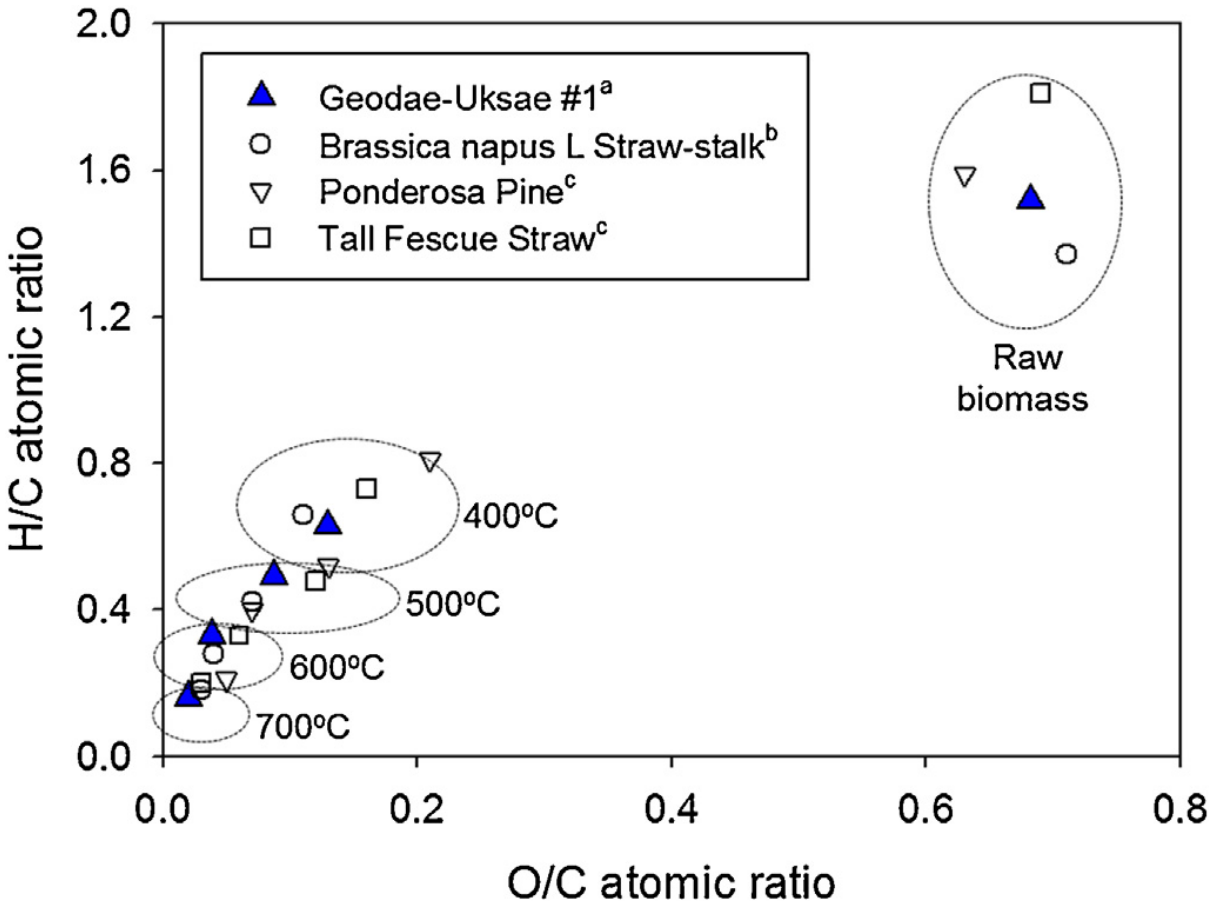


Fig. 4. Van Krevelen diagram for raw materials and biochars produced at different pyrolysis temperatures

Gasification

Gasification is a thermochemical partial oxidation process converting carbonaceous materials, such as biomass, coals, and plastic materials, to gaseous products using gasification agents (air, steam, oxygen, CO2 or gas mixture). In a gasification process, gaseous products (H_2, CO, CO_2, N_2, etc.), liquid products (tar and oil), and solid products

(char and ash) are formed. Because gasification is aimed at producing gaseous products, the yield of biochar is only approximately 5–10% of the raw biomass material mass, which is lower than that of fast pyrolysis (15–20%). Fig. 2 compares the product yields of slow pyrolysis, fast pyrolysis, and gasification. The mechanism of gasification can be divided into several steps, as shown below, but each step cannot be separated from the others clearly in terms of temperature and pressure.

Drying → Pyrolysis → Oxidation / Combustion → Gasification

(1) Drying

The moisture in biomass is evaporated in this step and the energy used for drying is not recovered. The moisture content of biomass varies according to the biomass material gasified. A separate drying step is required before the biomass is introduced into the gasifier when the moisture content is too high.

Table 1
Characteristics of biochar produced using different feedstock materials under different pyrolysis conditions.

Raw biomass	Temperature (°C)	Heating rate (°C/min)	Residence time (h)	Yield of biochar (%)	pH	Ash contents (%)	Fixed carbon (%)	C	C/H	C/O
Sewage sludge	450	5	–	53.0	80	50.7	–	36.0	1.15	7.50
	450	60	–	47.0	8.2	58.0	–	29.9	1.38	6.13
	650	5	–	47.0	9.0	60.3	–	30.8	2.13	9.78
	650	60	–	45.0	8.6	62.2	–	29.2	2.02	9.49
	850	5	–	45.0	11.7	62.3	–	33.0	3.93	25.89
	850	60	–	38.0	11.9	66.3	–	29.6	3.52	26.31
Conocarpus wastes	200	–	4	51.33	7.37	4.53	–	64.19	16.21	2.42
	400	–	4	31.86	9.67	5.27	–	76.83	27.15	5.43
	600	–	4	27.22	12.21	8.56	–	82.93	64.79	12.66
	800	–	4	23.19	12.38	8.64	–	84.97	137.05	17.45
Straw	200	–	1	84.95	5.34	11.90	33.63	45.57	7.90	1.19
	200	–	2	81.23	5.91	12.29	34.47	46.33	8.24	1.26
	200	–	4	78.24	6.11	12.78	34.72	46.52	8.46	1.29
	400	–	1	37.30	10.82	25.74	40.41	57.07	17.14	3.46
	400	–	2	35.91	10.86	27.54	42.66	57.59	17.89	3.67
	400	–	4	36.65	10.78	28.40	42.76	57.92	19.05	3.77
	600	–	1	32.48	10.93	32.33	49.87	59.17	38.42	5.36
	600	–	2	32.48	10.96	33.57	54.34	59.09	41.03	5.54
	600	–	4	30.89	10.99	34.31	55.37	60.80	45.71	5.73
Lignosulfonate	200	–	1	81.99	4.18	35.86	29.06	30.33	7.96	0.87
	200	–	2	78.93	4.56	36.15	28.79	31.07	8.61	0.95
	200	–	4	74.97	4.34	36.93	28.64	31.94	10.34	1.00
	400	–	1	58.51	9.75	45.61	33.56	33.58	18.45	1.20
	400	–	2	57.80	9.65	47.61	34.13	33.67	19.24	1.23
	400	–	4	57.24	9.35	49.83	32.28	33.60	21.27	1.25
	600	–	1	52.99	10.68	56.13	36.83	34.52	31.67	1.35
	600		2	48.12	12.5	58.12	35.56	34.60	31.45	1.24
	600		4	43.85	12.95	59.69	35.05	36.81	29.21	1.24
Bagasse	500	10	1	43.7	9.3	8.57	80.97	85.59	30.35	8.17
Cocopeat				62.9	10.3	15.90	67.25	84.44	29.32	7.24
Paddy straw				49.6	10.5	52.37	39.10	86.28	27.65	11.74
Palm kernel shell				53.5	6.9	6.86	80.85	87.85	30.19	10.79
Wood stem				42.6	9.5	2.28	83.47	89.31	34.75	12.17
Wood bark				50.3	9.6	12.84	68.66	84.84	27.11	8.32

(2) Pyrolysis

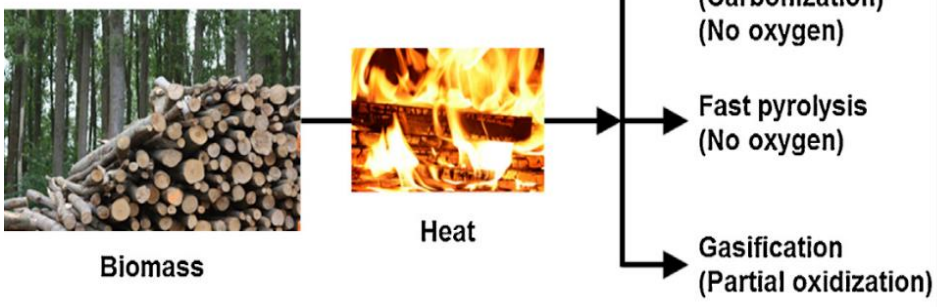
Pyrolysis takes place over the temperature range, 150–400°C, decomposing the thermally weak constituents of biomass, such as lignin, and producing char, gases and liquids.

$$\text{Biomass} + \text{Heat} \rightarrow \text{Char} + \text{Gases} + \text{Liquids}$$

Gaseous products formed during the pyrolysis step include H_2, CO, CO_2, H_2O, and small-molecular-mass hydrocarbons, such as CH_4. The liquid product is mostly mucous tar composed of small molecular-mass organic matter. The product composition depends on the reaction temperature, pressure, and temperature rising rate.

(3) Oxidation/combustion

Oxidation and combustion of some gas species and char are important sources of energy required for gasification reactions. The gasification agent provided into the gasifier reacts with combustible species, producing CO, CO_2 and H_2O, and with the char produced during the pyrolysis step, producing CO_2.



Product distribution (wt%)		
Solid	Liquid	Gas
35	30	35
10	70	20
10	5	85

Fig. 5. Comparison of the product distributions of pyrolysis and gasification of biomass

$$C + O_2 \rightarrow CO_2$$

$$H_2 + \tfrac{1}{2}\, O_2 \rightarrow H_2O$$

(4) Gasification

The char produced during the pyrolysis step is converted to CO, CH_4, and H_2 through various gasification reactions. The gasifiers, in which the gasification reactions take place, are divided into fixed bed reactors, moving bed reactors, fluidized bed reactors, and

entrained bed reactors depending on the way of contact between gasification agent and biomass. The parameters affecting the gasification reactions include the reaction temperature, gasification agent type, gasification agent–biomass ratio, and pressure. Taba et al. suggested that the temperature is the most important among the parameters directly affecting the gasification reactions. They reported that increasing temperature enhanced the production of H_2, CO, and carbon, while reducing the contents of CO_2, CH_4, hydrocarbons and tar. Gomez-Barea et al. also reported that the reduction of the gasification temperature in fluidized bed gasification resulted in reduced carbon conversion and an increased tar concentration in gas. Carbon conversion as well as the composition and heating value of the product gas also varies according to the gasification agent used in the gasification process. Tay et al. examined the effects of gasification agents on the characteristics of the char using a reducing gasification agent (H_2O) and oxidizing gasification agents (CO_2 and O_2). The ratio of the small and large aromatic ring structure of the aromatic compounds composing the char was lower and the contents of alkaline metals, such as Mg and Ca, in char were higher when H_2O was used.

Table 8: Comparison of the typical operation conditions for biochar production

Process	**Process temperature ℃**	**Residence time**	**Carbon content on solid product mass%**
Slow pyrolysis	~400	Minutes to days	95
Fast pyrolysis	~500	~1sec	74
Gasification	~800	~10-20 sec	-





Fig 6: a) Jute fibres of 2 to 4mm size b) Chopped fibres grinded in mixer grinder

6.1.4 Stock solution preparation:

For the preparation of a phosphate stock solution of 100 mg L^{-1}, Sodium fluoride (NaF) anddouble distilled water is used.

The molar mass of NaF is 41.99 gm mol^{-1} and the molar mass of F is 18.99 gm mol^{-1}

So, 18.99 gm F^- present in 41.99 gm NaF

1 gm F^- present in = (41.99/18.99×1) gm = 2.211 gm

100mg (0.1 gm) F^- present in = (2.211/0.1) gm = 0.2211 gm =221.1 mg NaF

To prepare 100 mg L^{-1} (100 ppm) fluoride stock, in 1000 ml distilled water, 0.2211 gm or 221.1 mg NaF has to be mixed. After the preparation of the stock solution, the concentration of fluoride must need to be checked for confirmation.

6.1.5 Preparation of Synthetic Solution:

2 mg L^{-1} Phosphate stock:

For preparation of 50ml 2mg/L conc. PO_4^{3-} synthetic solution

Initial volume (V_1) × initial conc.(S_1) = Final volume(V_2) × Final conc.(S_2)

or, $V_1 \times 100 = 50 \times 2$ [here Final conc.(V_2) = 50 ml and final conc. (S_2) = 2 mg L^{-1}]

or, $V_1 = 1$

So, 1 ml Phosphate stock has to mix with (50-1) ml =49 ml distilled water

5 mg L^{-1} Phosphate stock:

For preparation of 50ml 5mg/L conc. PO_4^{3-} synthetic solution

Initial volume (V_1) × initial conc.(S_1) = Final volume(V_2) × Final conc.(S_2)

or, $V_1 \times 100 = 50 \times 5$ [here Final conc.(V_2) = 50 ml and final conc. (S_2) = 5 mg L^{-1}]

or, $V_1 = 2.5$

So, 2.5 ml phosphate stock has to mix with (50-2.5) ml = 47.5 ml distilled water

10 mg L^{-1} Phosphate stock:

For preparation of 50ml 10mg/L conc. PO_4^{3-} synthetic solution

Initial volume (V_1) × initial conc. (S_1) = Final volume(V_2) × Final conc.(S_2)

or, $V_1 \times 100 = 50 \times 10$ [here Final conc.(V_2) = 50 ml and final conc. (S_2) = 10 mg L^{-1}]

or, $V_1 = 5$

So, 5 ml phosphate stock has to mix with (50-5) ml=45 ml distilled water.

20 mg L^{-1} Phosphate stock:

For preparation of 50ml 20mg/L conc. PO_4^{3-} synthetic solution

Initial volume (V_1) × initial conc. (S_1) = Final volume(V_2) × Final conc.(S_2)

or, $V_1 \times 100 = 50 \times 20$ [here Final conc.(V_2) = 50 ml and final conc. (S_2) = 20 mg L^{-1}]

or, $V_1 = 10$

So, 10 ml phosphate stock has to mix with (50-10) ml=40 ml distilled water.

30 mg L^{-1} Phosphate stock:

For preparation of 50ml 30mg/L conc. PO_4^{3-} synthetic solution

Initial volume (V_1) × initial conc. (S_1) = Final volume(V_2) × Final conc.(S_2)

or, $V_1 \times 100 = 50 \times 30$ [here Final conc.(V_2) = 50 ml and final conc. (S_2) = 30 mg L^{-1}]

or, $V_1 = 15$

So, 15 ml phosphate stock has to mix with (50-15) ml = 35 ml distilled water

40 mg L^{-1} Phosphate stock:

For preparation of 50ml 40mg/L conc. PO_4^{3-} synthetic solution

Initial volume (V_1) × initial conc. (S_1) = Final volume(V_2) × Final conc.(S_2)

or, $V_1 \times 100 = 50 \times 40$ [here Final conc.(V_2) = 50 ml and final conc. (S_2) = 40 mg L^{-1}]

or, $V_1 = 20$

So, 20 ml phosphate stock has to mix with (50-20) ml = 30 ml distilled water

Phosphate Conc. (mg L^{-1})	Stock Solution used (ml)	Distilled water used (ml)
2	1.0	49.0
5	2.5	47.5
10	5.0	45.0

20	10.0	40.0
30	15.0	35.0
40	20.0	30.0

Table 9: Phosphate Synthetic Stock preparation



Fig 7: Biochar from Jute

6.1.6 Method for measuring Phosphate concentration in water:

The spectrophotometry method is adopted for the analysis of phosphate in water. Hach Intellical ISEF121 combination fluoride ISE is used as a probe and HQ40d portable is used as a multimeter for measuring fluoride contamination in water. The following steps are followedin this method:

1. 50 mL of sample is added to a clean plastic beaker.
2. Then 1 pillow of TISAB (Total Ionic Strength Adjustment Buffer) is added to the sample.
3. After that Stir bar is added and the beaker is put on a magnetic stirrer and is stirred at a moderate rate.
4. The probe is put in the solution in such a way that probe did not touch the stir bar, bottom or sides of the container. Have to remove the air bubbles from under the probe tip.
5. The 'read' button is pushed when the measurement is stable,and the lock icon is shown. Then the reading is noted down.
6. After completion of every test the probe is washed using deionized distilled water and

the probe is dried using tissue paper.



Fig. 8: Ion Selective Electrode Method

6.1.7 Point of Zero Charge

The point of zero charge (PZC) is actually the pH at which the net surface charge of the adsorbent is equal to zero. At that pH, the charges of all positive sites become equal to negative ions.

$$pH = PZC$$

- ***Importance of PZC***

The PZC gives us information regarding ionization of the functional groups and contact of metal ions with the adsorbent in the aqueous system.

- ***Procedure***

The salt addition method is taken into account for the point of zero charge test. The following steps are followed for this experiment:

1. An aliquot of 40 mL of $NaNO_3$ (0.1M) is collected in ten different plastic conical flasks
2. Set the different pH values (3-12) of the solution with either HNO_3 (0.1 M) or NaOH (0.1 M) solution using a pH probe.
3. Then in each flask 1 gm of jute is added.
4. Then the flasks are inserted inside the shaker at 28$^{\circ}C$ and at a speed of 150 rpm for 24 hours.

5. After the equilibrium, the sample is filtered in plastic beakers.
6. At last, the pH of the filtered water is noted down.

6.1.8 Batch Study

Batch experiments were performed to determine the equilibrium time, kinetics and the selection of an isotherm. The batch experiment was performed following way:

1. ***Variation in Dosage***

   Fixed conc. of phosphate was taken in different plastic conical flasks and different dosage of biochar (0.5gm,1gm,1.5gm,2gm,2.5gm) were taken and flasks were shaken at a speed of 200 rpm for 4 hours to identify the removal efficiency of fluoride at a fixed temperature (28 ℃) and the experiment was repeated for fluoride concentration of 10 mg L^{-1}, 5 mg L^{-1}, 2 mg L^{-1}.

2. ***Variation in phosphate Concentration***

   Different concentrations of fluoride (2 mg L^{-1}, 5 mg L^{-1}, 10 mg L^{-1}, 15 mg L^{-1}, 20 mgL^{-1}, 25 mg L^{-1}, 30 mg L^{-1}, 40 mg L^{-1}, 50 mg L^{-1}) were taken in different plastic conical flasks and fixed 1 gm of biochar is added inside every flask and were shaken at a speed of 200 rpm at a fixed temperature (29℃) for 4 hours. The main purpose of the experiment was to check the efficiency of jute biochar at different phosphate concentration levels. This experiment was an important role in the isotherm study.

3. ***Variation in Agitation time***

   Fixed conc. (20 mg L^{-1}) of phosphate was taken in different plastic conical flasksand a fixed amount of biochar (1 gm) was added to every conical flask. Then inside the incubator, the flasks were shaken at a speed of 200 rpm at a fixed temperature (28℃). Every 50 min time interval one flask was taken out from the incubator and the final concentration was checked. The experiment was conducted for 300 minutes. This experiment had an important role in the kinetic analysis of adsorption.

4. ***Variation in pH***

   Fixed concentration (10 mg L^{-1}) phosphate was taken in different plastic conical flasks. Each conical flask was fixed at different pH level with help of 0.1N NaOH

and 0.1N HNO_3. pH levels are fixed from 4 to 10 and a fixed amount of biochar (1 gm) was added in every conical flask. After 5 hours of agitation witha speed of 200 rpm. The efficiency of removal of fluoride was observed atdifferent pH level. The test was conducted at 30 ℃.

6.2 ADSORPTION ISOTHERM FOR BATCH EXPERIMENT

Adsorption isotherm is the representation of the relationship between the adsorbate in the liquid phase and the adsorbate adsorbed on the surface of the adsorbent at equilibrium at an equilibrium state.

The amount of fluoride (adsorbate) adsorbed onto the adsorbents was determined from thefollowing equation:

$$q_e = \frac{(Ci - Ce)}{m} \times V$$

Where q_e is the fluoride adsorbed (mg g^{-1}); C_i is the initial concentration of fluoride (mg L^{-1}); Ce is the concentration of fluoride in solution at equilibrium time; V, solution volume (L); m, adsorbent dosage (gm)

The equilibrium adsorption isotherm is the most important to design the adsorption systems. For solid-liquid systems, several isotherms adsorption. The most important adsorption models are Langmuir, Freundlich, and Temkin adsorption isotherm models.

6.2.1 Langmuir Isotherm

The Langmuir adsorption model is based on the assumption that maximum sorption corresponds to a saturated monolayer of solute on the sorbent surface. This model also supposes that all the sorption sites are assumed to be identical, each site retains one molecule of the given compound and all sites are energetically and sterically independent of the sorbed quantity.

The Langmuir isotherm model equation is:

$$q = q_m \left(K_L \frac{Ce}{1 + KL\ Ce}\right)$$

The linear form of the Langmuir the equation can be described by:

$$\frac{Ce}{qe} = \frac{Ce}{qm} + \frac{1}{KL \times qm}$$

where C_e (mg L^{-1}) is the equilibrium concentration of the sorbate, q_e (mg g^{-1}) is the amount of adsorbate per unit mass of adsorbent, q_m (mg g^{-1}) is the maximum adsorption capacity (theoretical monolayer saturation capacity) and K_L (L mg^{-1}) is the Langmuir constant related to sorption capacity and rate of sorption.

The main characteristics of the Langmuir equation, constants K_L and qm, can be determined by plotting the $1/C_e$ versus $1/q_e$ curve for linearized form and the C_e versus q_e curve for non-linearized form.

The essential characteristics of the Langmuir isotherm can be expressed in terms of a dimensionless equilibrium parameter (R_L) defined by

$$R_L = \frac{1}{(1+KL \times Ci)}$$

The value of R_L indicates the type of the isotherm to be either favourable ($0<R_L<1$), unfavourable ($R_L>1$), linear ($R_L= 1$), or irreversible ($R_L=0$) [40].

6.2.2 Freundlich Model

The Freundlich isotherm model was originally an empirical nature but was later interpreted as sorption to heterogeneous surfaces or surface supporting sites of varied affinities. It is assumed that the stronger binding sites are occupied first and that binding strength decreases with increasing degree of site occupation. The Freundlich isotherm model can describe the adsorption of organic as well as inorganic compound on a wide variety of adsorbents [41].

The empirical form of the Freundlich isotherm model [42]:

$$q_e = K_F.C_e^{1/n}$$

where q_e is the adsorption (mg g^{-1}); C_e is the concentration of adsorbate in the solution (mg/L); K_F and n were empirical constants that are characteristics of the system, indicating the adsorption capacity and the adsorption intensity, respectively. The above equation can be linearized as the following form, also used to confirm the applicability of the model

$$\ln q_e = \ln K_F + \frac{1}{n \ln Ce}$$

K_F is the measure of sorption capacity and 1/n is the sorption intensity. The value of *n* of this model fell in the range of 1-10, indicating favorable sorption. The numerical value of $1/n < 1$ indicated that adsorption capacity was only slightly suppressed at lower equilibrium concentration [41].

The equilibrium data have further been analysed by using the linearized form of Freundlich isotherm, by plotting ln q_e versus ln C_e.

6.2.3 Temkin Isotherm

Temkin isotherm, which considers the effects of the heat of adsorption, decreases linearly with coverage of the adsorbate and adsorbent interactions. The Temkin isotherm has been used in the form as follows:

$$q_e = \frac{RT}{bt \times \ln (Kt)}$$

Where b_t is the Temkin constant related to the heat of sorption (J mol^{-1}), K_t is the Temkin isotherm constant (L mg^{-1}), R is the gas constant (8.314 J mol^{-1} K^{-1}) and T is the absolute temperature (in K). The parameters of Temkin model are determined by plotting the q_e versus lnC_e.

6.3 KINETICS STUDY FOR BATCH EXPERIMENT

For the determination of the adsorption rate constant, equilibrium adsorption capacity and adsorption mechanism of the experiment, a kinetic study was performed [43]. The kinetics of fluoride adsorption on both the laterite soils have been determined by using three different kinetic models, which are pseudo-first-order, pseudo-second-order and intra-particle diffusion models.

6.3.1 Pseudo-first-order model

This is the first equation for the sorption of liquid/solid system based on solid

capacity.[44] The following equation was considered for pseudo-first-order kinetic which was introduced by Lagergren [45,46]:

$$\frac{d(qt)}{dt} = k_1 (q_e - q_t)$$

The above equation can be integrated for following boundary conditions to obtain Equation

$t = 0$, $q_t = 0$, $t = t$, $q_t = q_t$

$$\ln (q_e - q_t) = \ln q_e - k_1.t$$

Where, q_e is the amount of solute on the surface of the sorbent at equilibrium, (mg g^{-1}), q_t is the amount of solute on the surface of the sorbent at time t, (mg g^{-1}), k_1 is the equilibrium rate constant of pseudo-first sorption, (L min^{-1}).

The pseudo-first-order rate constant (k_1) and theoretical equilibrium adsorption capacities (q_e) were calculated from a linear plot of ln ($q_e - q_t$) versus t.

6.3.2 Pseudo-second-order model

The pseudo-second-order model predicts the behavior over the whole adsorption time and is in agreement with the adsorption mechanism being the rate-controlling step. The pseudo-second-order rate equation is expressed as:

$$dq_t / dt = k_2 (q_e - q_t)^2$$

Where k_2 is the pseudo-second-order rate constant. After integration and applying boundary conditions, $t = 0$ to $t = t$ and $q_t = 0$ to $q_t = q_t$; the integrated form of above Eq. becomes:

$$t/q_t = 1/k_2.q_e^2 + t/q_e$$

The second-order rate constant k_2 and maximum adsorption capacity q_e have been calculated by plotting the graph of t/qt versus t for the linear pseudo-second-order model from the intercept and slope of this graph, respectively.

6.3.3 Intra-particle diffusion Model

Intra-particle diffusion model suggested by Weber and Morris , the initial rate of intra-particle diffusion can be calculated by plotting the q_t versus $t^{0.5}$ graph

$$q_t = k_{diff}. t^{1/2} + c$$

Where, q_t is amount of solute on the surface of the sorbent at time t, (mg gm^{-1}), k_{diff} is the intra-particle rate constant (mg gm^{-1} $min^{1/2}$), t is the time (min) and c (mg gm^{-1}) is a constant that gives an idea about the thickness of the boundary layer. If the Weber–Morris plot of q_t versus $t^{1/2}$ gives a straight line, then the adsorption process is controlled by intra-particle diffusion only.

6.4 ADSORPTION MODELS FOR COLUMN STUDY

Various practical features such as sorbent capacity, operating life span, regeneration time, and prediction of the time necessary play a vital role during the operation of the column using adsorption dynamics acquaintance and modeling. The column model study provides detailed conclusions about the mechanism of the process. The adsorption column is subjected to axial dispersion, external film resistance, and intra-particle diffusion resistance. To determine the adsorption mechanism of fluoride using laterite soil and to design the adsorption process in a dynamic regime, it is necessary to know the evolution of the residual concentration of the effluent in time. In this case, three models can be used, namely the Adams–Bohart, Yoon – Nelson, and Thomas models to analyze the breakthrough curves and for the prediction of the dynamic nature of the column.

6.4.1 Bohart–Adams Model

The Bohart–Adams Model is used to describe the first part of the column breakpoint curve. The Bohart–Adams equation is linearly expressed as:

$$\ln (C_t/C_o) = k_{BA}.Co.t – k_{BA}.N_0.(Z/F)$$

where: C_o is the effluent concentration, (mg L^{-1}); C_t is the effluent concentration,(mg L^{-1}); t is time, (min); k_{BA} is the kinetic constant of the Bohart-Adam model, (L mg^{-1} min^{-1}); F-is the linear velocity calculated by dividing the flow rate by the column section area,(cm min^{-1}); Z is the bed height of the column, (cm); N_0 is the saturation concentration, (mg L^{-1}). Bohart Adams Model model ln (C_t/C_o) is plotted against time (t).

6.4.2 Yoon–Nelson Model

The Yoon-Nelson Model is most commonly adopted to describe the breakpoint curve. It is a model used especially for the single-component system and does not require

information about the adsorbent, such as type, physical properties, or other characteristics. Yoon-Nelson equation is linearly expressed as:

$$\ln [C_t /(C_0-C_t)] = k_{YN}.t - \tau.k_{YN}$$

Where: C_t is the solution concentration at time t, (mg L^{-1}); C_0 is the initial solution concentration, (mg L^{-1}); k_{YN} is the rate constant, (min^{-1}); τ is the time required for 50% adsorbate breakthrough, (min). The parameters τ and k_{YN} can be obtained from the plot of the function $\ln[C_t/(C_0 - C_t)]$ against time (t).

6.4.3 Thomas Model

The Thomas model is the generally used model to describe the adsorption column performance and to establish breakthrough curves. It is frequently used to determine the adsorption capacity of the material. The Thomas equation is linearly expressed as:

$$\ln [(C_0/C_t)^{-1}] = (k_{TH}.q_{TH}.m/Q) - k_{Th}.C_0 .t$$

where: C_0 is the solution concentration in the effluent, (mgL^{-1}); C_t is the solution concentration at time t in the effluent, (mg L^{-1}); k_{TH} is the Thomas rate constant, (L min^{-1} mg^{-1}); q_{TH} is the equilibrium compounds uptake per gm, (mg gm^{-1}); m is the mass of adsorbent, (gm); Q is the flow rate, (mL min^{-1}). k_{TH} and q_{TH} are determined by plotting the $\ln [(C_0/C_t)^{-1}]$ against the time (t) graph.

CHAPTER- 6

7.1 RESULT & DISCUSSION

7.2 Analysis of phosphate in different concentration

Phosphate adsorption percentage in different concentration is shown in table 10 when the dosage of biochar is 0.5 gm and it is rotated at 200 rpm for 4 hrs.

Phosphate conc. Mg/L	Adsorption value	Adsorption %
2	1.77	11.5
5	4.46	10.8
10	4.26	57.4
15	4.42	70.5
20	4.48	77.6
30	4.56	84.8

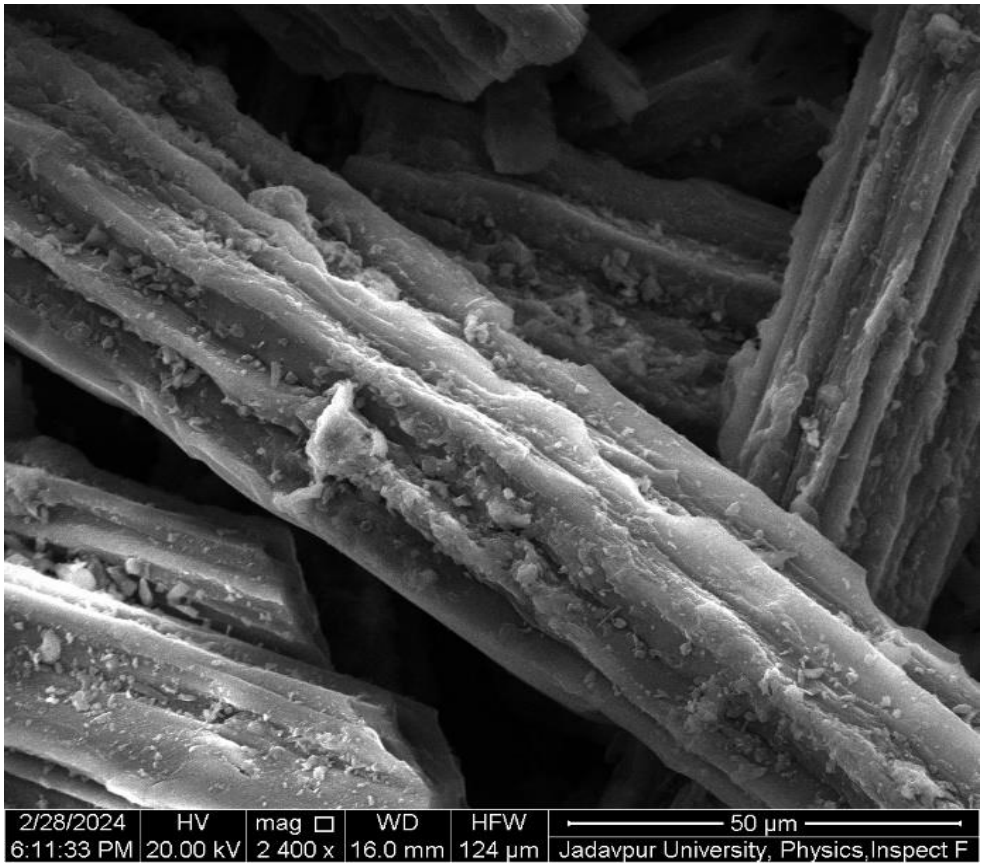
Table 10: Phosphate adsorption at different concentration

7.2 CHARACTERIZATION STUDY OF THE ABSORBENT

7.2.1 FESEM & EDX Study:

The surface characterization of biochar is very important, which is based on its chemical structure and morphology. The information on the surface chemistry of biochar could be useful in examining the adsorption mechanism and nutrients recovery process, since nutrient compositions are mainly retained by oxygen-containing surface functional groups (carboxyl, hydroxyl, phenolic) of biochars. Nowadays, various techniques can be employed to study the surface morphology and composition of biochars [*Gai et al., 2014*]. With regarding to the surface morphology, SEM equipped with EDX can be used for analyzing surface structure and elemental composition, such as N, H, C, and S of biochar. For example, *Karunanithi et al.* (2017) investigated that the SEM image of biochar (soybean stover) exhibited a large number of cracks and improved porous structures owing to destruction and elimination of volatile compounds during pyrolysis (Fig. 2a). Fig. 2b showed that after adsorption process the porous structure of soybean stover biochar was

filled with the phosphate ions confirming the phosphate adsorption. Moreover, the EDX analyses of biochar showed that biochar had higher percentage of C, Mg, and Ca while lower amount of S and P [*Karunanithi et al., 2017*].



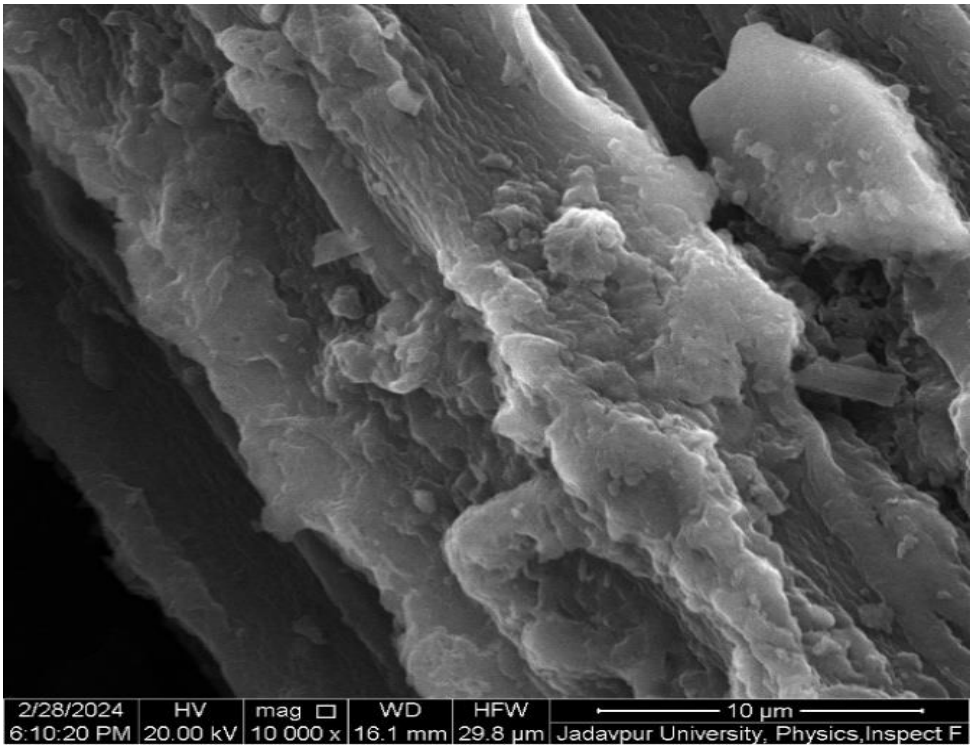


Fig 9: SEM image of Jute Biochar

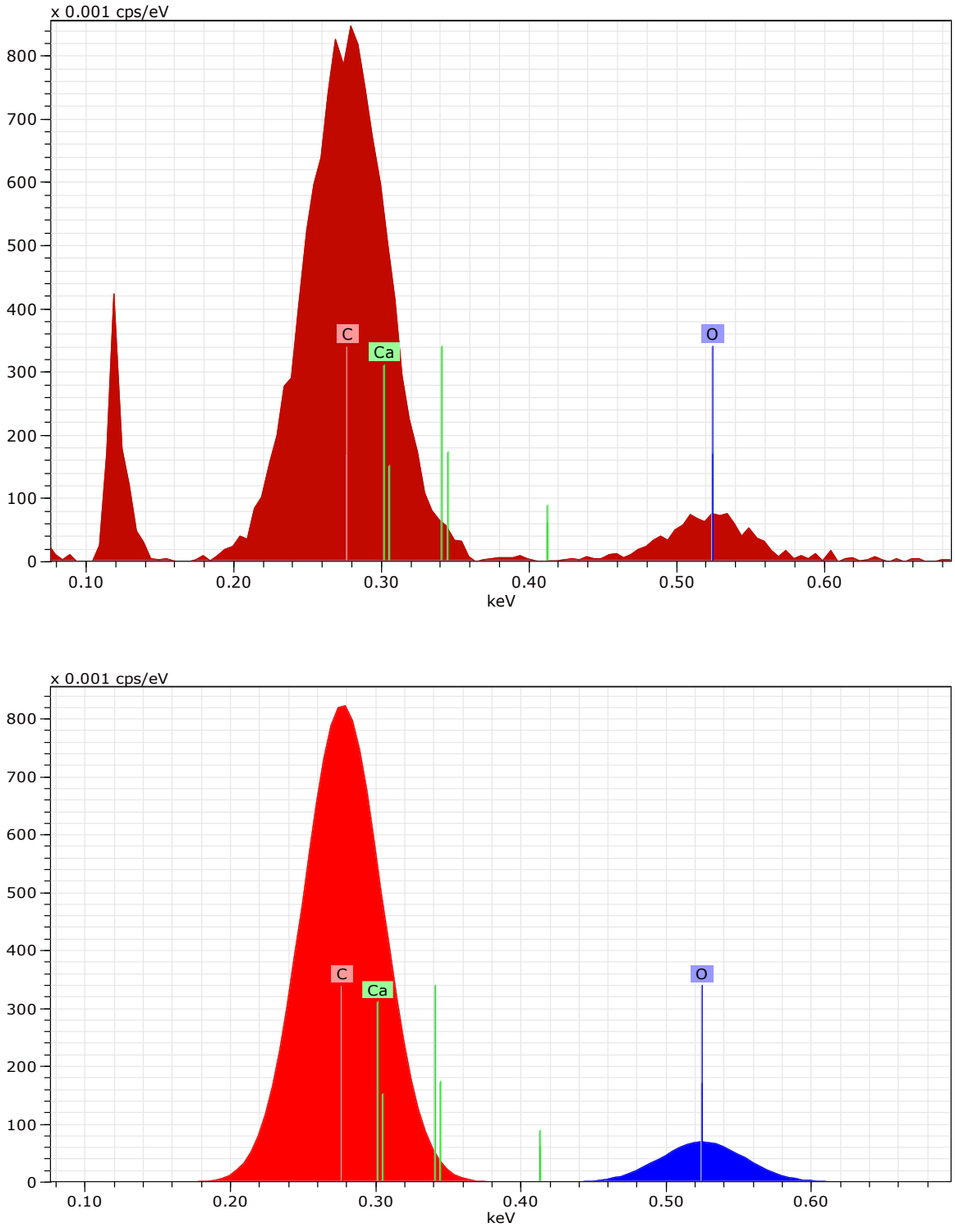


Fig 10: EDX data of Jute biochar

7.2.2 FTIR Study:

To analyze the functional groups on the surface of the untreated and treated jute fibers, FTIR spectroscopy measurements (NEXUS670, Thermo Instrument, USA) in the mid infrared (4000–500 cm^{-1}) were performed. The specimens must be dried sufficiently to avoid the disturbance of water. FTIR spectra were recorded on powder samples, which were obtained from the cut jute fibers, dispersed in dry KBr using

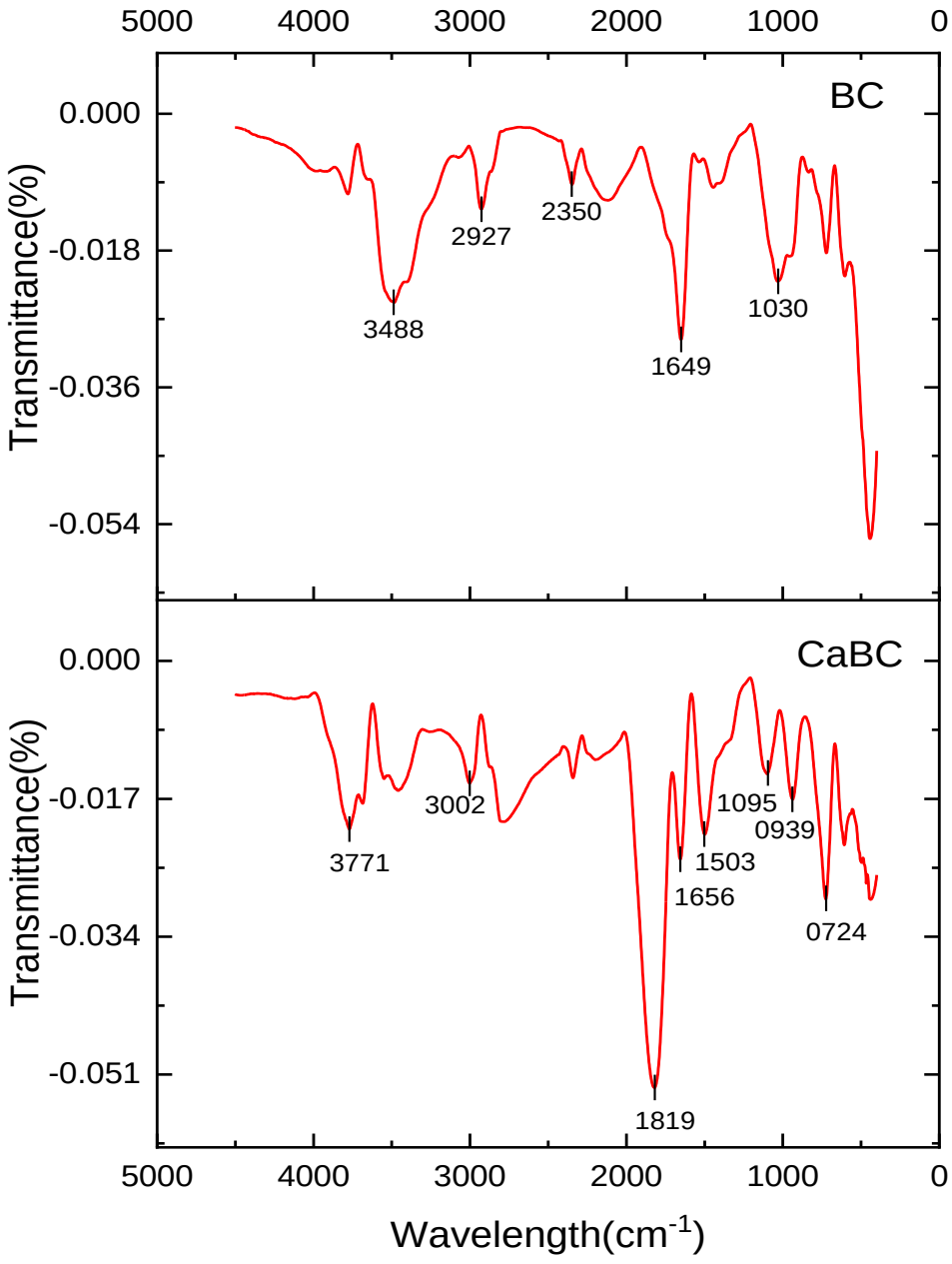


Fig 11: Fourier Transformation Infrared (FTIR) spectral data of Jute biochar and Ca

modified jute biochar

Bruker IFS/66v. Moreover, the fiber must be finely cut into segments (length is<1 mm) via a special cutting machine before being mixed with potassium bromide, because it is so easy for Infrared light wave to be reflected by long fibers that the analysis sensitivity and precision will be decreased enormously. After the preparation, the FTIR spectra of original and treated Jute fibers were recorded on a Nicolet 5700 spectrometer using potassium bromide pellet technique and the scanning was carried out from 500 cm^{-1} to 4000 cm^{-1}. Absorbance (A) is the flip-side of transmittance and states how much of the light the sample absorbed. It is also referred to as "optical density." Absorbance is calculated as a logarithmic function of T: A = log10 (1/T). If the transmittance is high then the absorbance will be low. The peak at 1649 cm^{-1} indicates that double bond carbon (C = C) or olefinic compound. The range between 1850 to 1650 cm^{-1} indicates the presence of carbonyl compound. The peak value 1819 cm^{-1} informing active carbonyl groups such as anhydrides, halide acids, or halogenated carbonyl, or ring-carbonyl carbons, such as lactone, or organics carbonate. And the peak value of 1656 cm^{-1} indicating amides or carboxylates functional group. In jute biochar, presence of 1030 cm^{-1} exhibits the presence of phosphate ions similarly, after it is treated with Ca, phosphate ion increases to the peak value of 1095 cm^{-1}.

7.3 DISCUSSION:

In various parts of India, jute, is readily available. The use of it as anadsorbent to remove phosphate from drinking water can be recommended. Adsorbents used in construction of dephosphatation units incur the cost of adsorbents, activation and processing, as well as transportation costs. As adsorbent, jute is widely available, and only transportation costs are necessary since it does not require any typical processing or activation. In this study application of jute of two different samples gave good results. From the batch experiment data, it can be said jute biochar exhibits a satisfactory efficiency for the removal of phosphate. It can be achieved more than 90% if a certain amount (1gm) of biochar is applied at 28°C and agitation speed 200 rpm.. The removal efficiency differs because of the difference of agitation time (reported 195 min) and temperature differences (reported 30°C). In this study, point of zero charge was found at pH 5.67. Sarkar *et al.*2006 was reported point of zero charge at pH 3.98. The difference is because of different amounts of other oxides present along with silica and alumina. With the increase of agitation time the removal.

.

CHAPTER- 7

8.1 CONCLUSION & LIMITATIONS

8.1.1 Conclusion:

In conclusion, the application of biochar for removing phosphate from water shows great promise as an effective and sustainable water treatment method. Biochar, with its unique physical and chemical properties, has demonstrated remarkable adsorption capabilities, efficiently binding with heavy metals and reducing their concentrations in contaminated water.

By harnessing the adsorption mechanism of biochar, we can mitigate the adverse effects of heavy metal contamination on human health and the environment. The process is environmentally friendly and cost-effective, making it an attractive alternative to conventional water treatment methods.

While biochar shows significant potential, it is essential to consider various factors that can affect its adsorption efficiency, such as temperature, pH, contact time, and the characteristics of the biochar itself. Continued research and development are necessary to optimise the use of biochar in water remediation.

Despite its numerous advantages, literature reviews from researchers are there on the adsorption studies of phosphate, nitrate and iron using biochar. From there following research gaps are found:

- Applications of a new form of biochar in the removal technology
- Application of biochar for phosphate removal from water is very few.
- To use deashed biochar in the removal process of phosphate, nitrate and iron.
- To check the effect of different structural and textural characteristics of the available biochar in contaminant removal.

- To check the applicability of biochar sludge from nitrate and phosphate removal to enhance soil fertility.

Looking to the future, the application of biochar for removing phosphate from water holds great promise for sustainable water management. Continued research, technological advancements, and innovative approaches will undoubtedly lead to more effective and widespread implementation of biochar-based water treatment solutions.

In conclusion, the integration of biochar into water treatment strategies offers a ray of hope in combating heavy metal pollution, paving the way for a cleaner and healthier environment for current and future generation.

8.1.2 Limitation of the study

Jute is a low cost natural filter medium for phosphate removal, at small scale water treatment. However it is worthwhile investigating the application of this technology at medium scale. Thereby large scale application and optimisation of parameters is required which has not been considered in this study because of short tenure of the course.

8.1.3 Future works

It was concluded that the use of jute fibres for phosphate removal is very promising on a domestic scale where drinking, even in the presence of another ions such as Cl^- ; SO_4^{2-}, NO_3^- etc. But such ions have some health implications which whose concentrations is also needed to be optimised in future study. More optimisation for the fixed bed columns study is required with analysis of the regeneration of repetitive cycles of jute for phosphate removal.

REFERENCES

[1] I. Langmuir, The constitution and fundamental properties of solids and liquids. Part I. Solids, J. Am. Chem. Soc. 38 (1916) 2221–2295.

[2] H.M.F. Freundlich, Über die Adsorption in Lösungen, Z. für Phys. Chem. 57A (1906) 385–470 Google Scholar.

[3] S.K. Lagergren, About the theory of so-called adsorption of soluble substances, Sven. Vetenskapsakad. Handingarl 24 (1898) 1–39.

[4] L. Anah, N. Astrini, Isotherm adsorption studies of Ni (II) ion removal from aqueous solutions by modified carboxymethyl cellulose hydrogel, In IOP
Conference Series: Earth and Environmental Science (2018) (Vol. 160, No. 1, p. 012017). IOP Publishing.

[5] Kamble SM. Water pollution and public health issues in Kolhapur city in Maharashtra. International Journal of Scientific and Research Publications. 2014;4(1):1-6

[6] Desai N. SmtVanitaben. A study on the water pollution based on the environmental problem. Indian Journal of Research. 2014;3(12):95-96

[7] Moore JW, Moore EA. Resources in environmental chemistry. I. An annotated bibliography of the chemistry of pollution and resources. Journal of Chemical Education. 1976;53(3):167

[8] Sankhla et al. Impact of variation in climatic changes in concentration of Lead & Nickel in Yamuna River Water, Delhi, India. Materials Today: Proceedings. Elsevier; 2022

[9] Baird RB et al. Standard Methods for the Examination of Water and Wastewater. Vol. 23. Washington, DC: American Public Health Association; 2017

[10] Sankhla et al. Seasonal Variations of Lead and chromium concentration in the water samples from Yamuna River in Delhi, India. Iranian Journal of Toxicology. 2021;15(2):109-114

[11] Cempel M, Nikel GJPJS. Nickel: A review of its sources and environmental toxicology. Polish Journal of Environmental Studies. 2006;15(3):375-382

[12] Li Y et al. The distribution of dissolved lead in the coastal waters of the East China Sea. Marine Pollution Bulletin. 2014;85(2):700-709

[13] Li P et al. Mercury pollution in Asia: A review of the contaminated sites. Journal of Hazardous Materials. 2009;168(2-3):591-601

[14] Ho Y et al. Industrial discharge and their effect to the environment. Industrial Waste, Intech. 2012:1-39

[15] Kowalski A, Siepak M, Boszke L. Mercury Contamination of Surface and Ground Waters of Poznań, Poland. Polish Journal of Environmental Studies. 2007;16(1)

[16] V. Chakraborty, P. Das, P.K. Roy, Graphene oxide–coated pyrolysed biochar from waste sawdust and its application for treatment of cadmium-containing solution: batch, fixed-bed column, regeneration, and mathematical modelling, Biomass Conv. Bioref. (2021), https://doi.org/10.1007/s13399-020-01153-7.

[17] M. Charoenchai, S. Tangbunsuk, Effect of ternary polymer composites of macroporous adsorbents on adsorption properties for heavy metal removal from aqueous solution, Environ. Sci. Pollut. Res. (2022), https://doi.org/10.1007/ s11356-022-21701-0.

[18] J.P. Simonin, On the comparison of pseudo-first order and pseudo-second order rate laws in the modeling of adsorption kinetics, Chem. Eng. J. 300 (2016) 254–263, https://doi.org/10.1016/j.cej.2016.04.079.

[19] H. Moussout, H. Ahlafi, M. Aazza, H. Maghat, Critical of linear and nonlinear equations of pseudo-first order and pseudo-second order kinetic models, Karbala Int. J. Mod. Sci. 4 (2) (2018) 244–254, https://doi.org/10.1016/ j.kijoms.2018.04.001.

[20] E.H. Lee, R. Park, H. Kim, S.H. Park, S.C. Jung, J.K. Jeon, S.C. Kim, Y.K. Park, J. Ind. Eng. Chem. 37 (2016) 18.

[21] T.U. Han, Y.M. Kim, C. Watanabe, N. Teramae, Y.K. Park, S. Kim, Y. Lee, J. Ind. Eng. Chem. 32 (2016) 345.

[22] A. Demirbas, J. Anal. Appl. Pyrolysis 72 (2004) 243.

[23] G. Chen, J. Andries, Z. Luo, H. Spliethoff, Energy Convers. Manage. 44 (2003) 1875.

[24] A.I. Mohammad, A.E. Abdulrasoul, H. Ahmed, N. Mahmoud, U.R.A. Adel, Bioresour. Technol. 131 (2013) 374.

[25] Z.A. Abu El-Rub, E.A. Bramer, G. Brem, Fuel 87 (2008) 2243.

[26] FAO, World Fertilizer Trends and Outlook to, Summary Report in, Food and Agriculture

[27] O Vikrant, K., Kim, K. H., Ok, Y. S., Tsang, D. C., Tsang, Y. F., Giri, B. S., & Singh, R. S. (2018). Engineered/designer biochar for the removal of phosphate in water and wastewater. *Science of the Total Environment*, *616*, 1242-1260.rganization of the United Nations, Rome, 2020, p. 2017.

[28] Ramola, S., Belwal, T., Li, C. J., Liu, Y. X., Wang, Y. Y., Yang, S. M., & Zhou, C. H. (2021). Preparation and application of novel rice husk biochar–calcite composites for

phosphate removal from aqueous medium. *Journal of Cleaner Production*, *299*, 126802.

[29] Wang, B., Lian, G., Lee, X., Gao, B., Li, L., Liu, T., ... & Zheng, Y. (2020). Phosphogypsum as a novel modifier for distillers grains biochar removal of phosphate from water. *Chemosphere*, *238*, 124684.

[30] Yao, Y., Gao, B., Chen, J., Zhang, M., Inyang, M., Li, Y., ... & Yang, L. (2013). Engineered carbon (biochar) prepared by direct pyrolysis of Mg-accumulated tomato tissues: characterization and phosphate removal potential. *Bioresource technology*, *138*, 8-13.

[31] Li, J., Cao, L., Li, B., Huang, H., Yu, W., Sun, C., ... & Young, B. (2023). Utilization of activated sludge and shell wastes for the preparation of Ca-loaded biochar for phosphate removal and recovery. *Journal of Cleaner Production*, *382*, 135395.

[32] Ou, W., Lan, X., Guo, J., Cai, A., Liu, P., Liu, N., ... & Lei, Y. (2023). Preparation of iron/calcium-modified biochar for phosphate removal from industrial wastewater. *Journal of Cleaner Production*, *383*, 135468.

[33] Jiang, D., Chu, B., Amano, Y., & Machida, M. (2018). Removal and recovery of phosphate from water by Mg-laden biochar: Batch and column studies. *Colloids and Surfaces A: Physicochemical and Engineering Aspects*, *558*, 429-437.

[34] Trazzi, P. A., Leahy, J. J., Hayes, M. H., & Kwapinski, W. (2016). Adsorption and desorption of phosphate on biochars. *Journal of environmental chemical engineering*, *4*(1), 37-46.

[35] Zheng, Y., Zimmerman, A. R., & Gao, B. (2020). Comparative investigation of characteristics and phosphate removal by engineered biochars with different loadings of magnesium, aluminum, or iron. *Science of the Total Environment*, *747*, 141277.

[36] Ajmal, Z., Muhmood, A., Dong, R., & Wu, S. (2020). Probing the efficiency of magnetically modified biomass-derived biochar for effective phosphate removal. *Journal of environmental management*, *253*, 109730.

[37] Bock, E., Smith, N., Rogers, M., Coleman, B., Reiter, M., Benham, B., & Easton, Z. M. (2015). Enhanced nitrate and phosphate removal in a denitrifying bioreactor with biochar. *Journal of environmental quality*, *44*(2), 605-613.

[38] Zhang, M., He, M., Chen, Q., Huang, Y., Zhang, C., Yue, C., ... & Mu, J. (2022). Feasible synthesis of a novel and low-cost seawater-modified biochar and its potential application in phosphate removal/recovery from wastewater. *Science of The Total Environment*, *824*, 153833.

[39] Zhang, M., Gao, B., Yao, Y., & Inyang, M. (2013). Phosphate removal ability of

biochar/MgAl-LDH ultra-fine composites prepared by liquid-phase deposition. *Chemosphere*, *92*(8), 1042-1047.

[40] Peng, G., Jiang, S., Wang, Y., Zhang, Q., Cao, Y., Sun, Y., ... & Wang, L. (2020). Synthesis of Mn/Al double oxygen biochar from dewatered sludge for enhancing phosphate removal. *Journal of cleaner production*, *251*, 119725.

[41] Zhang, Z., Yan, L., Yu, H., Yan, T., & Li, X. (2019). Adsorption of phosphate from aqueous solution by vegetable biochar/layered double oxides: fast removal and mechanistic studies. *Bioresource technology*, *284*, 65-71.

[42] Nakarmi, A., Bourdo, S. E., Ruhl, L., Kanel, S., Nadagouda, M., Alla, P. K., ... & Viswanathan, T. (2020). Benign zinc oxide betaine-modified biochar nanocomposites for phosphate removal from aqueous solutions. *Journal of Environmental Management*, *272*, 111048.

[43] Nobaharan, K., Bagheri Novair, S., Asgari Lajayer, B., & van Hullebusch, E. D. (2021). Phosphorus removal from wastewater: The potential use of biochar and the key controlling factors. *Water*, *13*(4), 517.

[44] Dai, Y., Wang, W., Lu, L., Yan, L., & Yu, D. (2020). Utilization of biochar for the removal of nitrogen and phosphorus. *Journal of Cleaner Production*, *257*, 120573.

[45] Tao, X., Huang, T., & Lv, B. (2020). Synthesis of Fe/Mg-biochar nanocomposites for phosphate removal. *Materials*, *13*(4), 816.

[46] Xu, Q., Chen, Z., Wu, Z., Xu, F., Yang, D., He, Q., ... & Chen, Y. (2019). Novel lanthanum doped biochars derived from lignocellulosic wastes for efficient phosphate removal and regeneration. *Bioresource technology*, *289*, 121600.

[47] Alberto, D. R., Tyler, A. C., & Trabold, T. A. (2021). Phosphate adsorption using biochar derived from solid digestate. *Bioresource Technology Reports*, *16*, 100864.

[48] Wang, P., Zhi, M., Cui, G., Chu, Z., & Wang, S. (2021). A comparative study on phosphate removal from water using Phragmites australis biochars loaded with different metal oxides. *Royal Society Open Science*, *8*(6), 201789.

[49] Peng, Y., Sun, Y., Sun, R., Zhou, Y., Tsang, D. C., & Chen, Q. (2019). Optimizing the synthesis of Fe/Al (Hydr) oxides-Biochars to maximize phosphate removal via response surface model. *Journal of Cleaner Production*, *237*, 117770.

[50] Buates, J., & Imai, T. (2020). Biochar functionalization with layered double hydroxides composites: Preparation, characterization, and application for effective phosphate removal. *Journal of Water Process Engineering*, *37*, 101508.